COORDINATION
CHEMISTRY
REVIEWS

ELSEVIER

Mechanistic studies of some macrocyclic complexes

Stephen F. Lincoln

Department of Chemistry, University of Adelaide, Adelaide, SA 5005, Australia

Contents

Abstract

A review of recent research carried out at Adelaide in three areas of macrocyclic complex chemistry: (i) coronates, cryptates and related metal complexes; (ii) metal complexes of pendant arm macrocyclic ligands; and (iii) metallocyclodextrins is presented, and the relationship between complex stability, lability and structure is explored. © 1997 Elsevier Science S.A.

1. Introduction

The pioneering research of the Nobel Laureates for 1987, Pedersen [1,2], Lehn [3–7] and Cram [8–10] generated the coronands, cryptands, spherands and cavitands, and has stimulated a great and enduring interest in the selective complexation of metal ions and other species by macrocyclic ligands. Contemporaneously, the characterization of ionophoric antibiotics [11,12] and the inclusion complexes of the cyclodextrins [13–19] gave new insights into the selective complexation processes of naturally occurring macrocycles. Meanwhile, the syntheses of the tetraaza macrocycles cyclen [20] and cyclam [21] generated a new impetus to the study of transition metal complexes [22], and subsequently the attachment of pendant arms with oxygen donor groups to these ligands extended their complexing abilities to the alkali metal and lanthanide ions [23–27].

This evolution of the chemistry of macrocyclic complexes provided great stimula-

tion to our research in Adelaide, and in this review we discuss some of our endeavours together with related research of others in three main areas: coronates, cryptates and related complexes; metal complexes of pendant arm macrocyclic ligands; and metallocyclodextrins. A linking theme throughout is the relationship between complex stability, lability and structure, and the mechanistic insight which accrues. Readers seeking a more comprehensive coverage are directed to some excellent reviews of macrocyclic chemistry [22,28–31] in addition to the references cited above.

2. General aspects of coronates and cryptates

The chemistry of the coronands and cryptands (Fig. 1) which are remarkable for their ability to complex alkali and alkaline earth metal ions in addition to other metal ions to form coronates, $[M(coronand)]^{m+}$, and cryptates, $[M(cryptand)]^{m+}$, respectively, has been widely reviewed [1–7,29–31]. However, because of the extraordinary extent of this chemistry, it is necessary to briefly review some of its salient aspects to place our research in context.

Much discussion of coronand and cryptand solution chemistry revolves around their structures determined by X-ray crystallography. The coronands, as exemplified by 18C6 possess puckered structures in which the oxygens are in a common plane, and from which their name originates [32]. Coronate structures are exemplified by $[K(18C6)]^+$ where the coronand ring opens to accommodate K^+ in the mean plane of the coordinating oxygens [33], while in $[Na(18C6)]^+$ the coronand assumes a conformation with one oxygen out of the mean plane of the other five to partially encapsulate Na^+ [34]. The structure adopted by $[K(18C6)]^+$ is attributable to K^+, whose eight-coordinate radius (r_M) is 151 pm [35], optimising bonding distances by fitting into the 18C6 ring, whose hole radius is estimated at 130 pm from Cory–Pauling–Koltun models [36,37] and 140.5 pm from crystallographic data [38], while interacting with two SCN^- above and below the ring. These distances are optimised in $[Na(18C6)]^+$ through distortion of the ring to accommodate the smaller seven-coordinate Na^+ ($r_M = 112$ pm) which is also coordinated to a water. In $[Na(15C5)]^+$ [39] seven-coordinate Na^+ is out of the plane of the 15C5 ring, whose hole radius is estimated to be 85 pm from Cory–Pauling–Koltun models and 103.6 pm from crystallographic data [36–38], and is also coordinated to one SCN^- and a water. Thus, although M^+ and coronand hole size are major compo-

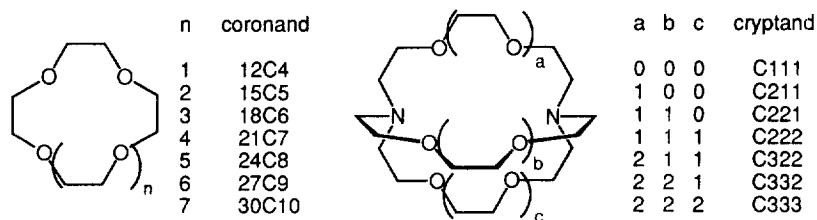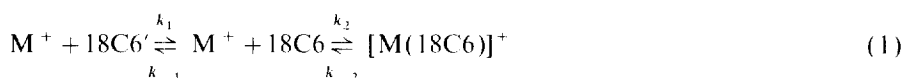|	n	coronand		a	b	c	cryptand
	1	12C4		0	0	0	C111
	2	15C5		1	0	0	C211
	3	18C6		1	1	0	C221
	4	21C7		1	1	1	C222
	5	24C8		2	1	1	C322
	6	27C9		2	2	1	C332
	7	30C10		2	2	2	C333

Fig. 1. Schematic representations of coronands and cryptands.

nents determining coronate structure, interactions with counter ions and water play a role in the crystalline state, and it is anticipated that similar factors are important in solution.
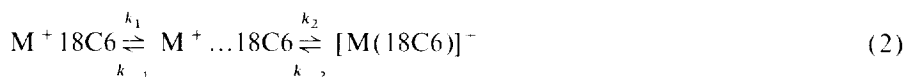
Because of the bicyclic structure of cryptands, the size relationship between M^+ and the cryptand cavity is more clear cut than is the analogous relationship for the coronands. Thus, in the crystalline state, cryptates may exist in an *inclusive* form where the metal ion is at the centre of the cryptand cavity, and an *exclusive* form where the metal ion is too large to fit into the cavity and resides on one face of the cryptand. Such inclusive cryptates are exemplified by $[Li(C211)]^+$ [40], $[Na(C221)]^+$ [41], and $[Na(C222)]^+$ [40] and its Rb^+ and Cs^+ analogues [42]. (Although eight-coordinate Rb^- and Cs^+ are substantially larger than the estimated C222 cavity size, this cryptand is sufficiently flexible to accommodate them.) Exclusive cryptates are exemplified by $[Na(C211)]^+$ [43] and $[K(C221)]^+$ [41].

In the formation of macrocyclic metal complexes the solvation energy of M^+ and the macrocyclic ligand, the hardness or softness of M^+ and the macrocycle donor atoms [44,45], the number of macrocycle donor atoms, the relative sizes of M^+ and the cavity formed by the macrocycle, and the conformational changes accompanying complexation all affect stability. The coronand 18C6 shows a substantial selectivity in complexing alkali metal ions as is exemplified by the variation of the stability of $[M(18C6)]^+$ in water for which $\log(K/dm^3 \, mol^{-1}) = 0.80$, 2.03, 1.56 and 0.99, where $M^+ = Na^+$, K^+, Rb^+ and Cs^+, respectively, at 298.2 K where K is the formation constant [46]. A similar selectivity is found in methanol, as indicated by $\log(K/dm^3 \, mol^{-1}) = 4.42$, 6.15, 5.35 and 4.37 where the stabilities are higher because of the decreased ability of this solvent to compete with 18C6 for M^+ [47]. The increased stability of $[K(18C6)]^-$ in methanol by comparison with that of the K^+ complex of pentaethylene glycol, $CH_3O((CH_2)_2O)_5CH_3$, the linear analogue of 18C6 for which $\log(K/dm^3 \, mol^{-1}) = 2.20$ [37], typifies the generally greater stability of the coronates compared with the complexes of their linear polyether analogues. This is termed the "macrocyclic effect". The smaller 15C5 is selective for Na^+ as indicated by $\log(K/dm^3 \, mol^{-1}) = 4.03$, 4.87, 3.78, 3.74 and 3.39, where $M^+ = Li^+$, Na^+, K^+, Rb^+ and Cs^+, respectively, at 298.2 K in propylene carbonate [48]. The corresponding values for 18C6 are 2.70, 4.55, 6.08, 5.33 and 4.48. This change in selectivity may be partly attributed to the change in coronand cavity radius which increases for 14C4, 15C5, 18C6 and 21C7 in the sequence 60, 85, 130 and 170 pm as estimated from Corey–Pauling–Koltun models [36,37]. However, change in solvent can sometimes cause changes in macrocyclic selectivity for metal ions as is discussed in Sections 3 5.

The formation of a coronate requires sequential desolvation and conformational changes, but more than two steps are seldom kinetically characterised. Acoustic studies of $[M(18C6)]^+$ in water have been interpreted in terms of a mechanism where 18C6 assumes a conformation appropriate to complexation of M^+ (k_1/k_{-1}) prior to the complexation step (k_2/k_{-2})

$$M^+ + 18C6' \underset{k_{-1}}{\overset{k_1}{\rightleftharpoons}} M^+ + 18C6 \underset{k_{-2}}{\overset{k_2}{\rightleftharpoons}} [M(18C6)]^+ \tag{1}$$

For the first equilibrium $k_1 = 6.3 \times 10^8$ s^{-1} and $k_{-1} = 1 \times 10^7$ s^{-1} at 298.2 K, and for the second $10^{-8}k_2 = 0.8$, 2.2, 4.3, 4.4 and 4.3 dm^3 mol^{-1} s^{-1} and $10^{-7}k_{-2} = 6$, 3.4, 0.37, 1.2 and 4.4 s^{-1} for Li$^+$, Na$^+$, K$^+$, Rb$^+$ and Cs$^+$, respectively [49]. A different model has been proposed for [M(18C6)]$^+$ in methanol where the initial step is the formation of an encounter complex (k_1/k_{-1}) where 18C6 resides in the second coordination sphere of Na$^+$ which is followed by desolvation and conformational change in the second stage (k_2/k_{-2})

$$\mathrm{M^+\,18C6} \underset{k_{-1}}{\overset{k_1}{\rightleftharpoons}} \mathrm{M^+\ldots 18C6} \underset{k_{-2}}{\overset{k_2}{\rightleftharpoons}} [\mathrm{M(18C6)}]^- \qquad (2)$$

The (k_1/k_{-1}) equilibrium lies to the right and is not kinetically characterised by the acoustic technique used, and $10^{-8}k_2 = 0.6$, 2.8 and 1.8 s^{-1} for Li$^+$, Na$^+$ and K$^+$, respectively, at 298.2 K [50]. A major difference between the mechanisms is that in the first 18C6 assumes an appropriate conformation before M$^+$ complexation and vice-versa in the second. Nevertheless, in the absence of M$^+$, the conformational equilibrium

$$\mathrm{18C6'} \underset{k_{-0}}{\overset{k_0}{\rightleftharpoons}} \mathrm{18C6} \qquad (3)$$

for which $k_0 \sim 2 \times 10^7$ s^{-1} and $k_{-0} = 2.04 \times 10^9$ s^{-1} is detected in methanol [50]. Irrespective of differences in mechanistic interpretation, these studies indicate that some of the coronand and coronate rate processes are rapid and are solvent dependent. The latter effect is found in our ^{23}Na NMR study of the Na$^+$ exchange

$$\mathrm{Na^+ + 18C6} \underset{k_d}{\overset{k_c}{\rightleftharpoons}} [\mathrm{Na(18C6)}]^+ \qquad (4)$$

where $10^{-9}k_c = >4.1$, 1.5 and 0.1 dm^3 mol^{-1} s^{-1} and $10^{-4}k_d = 43.4$, 7.2 and 1.03 s^{-1} in acetone, methanol and pyridine at 298.2 K, respectively [51]. The k_d decomplexation step is a different and slower step by comparison with the k_{-2} step detected by the acoustic studies, and probably represents an early stage in the resolution and conformational changes leading to decomplexation of [Na(18C6)]$^+$. The complexation $k_c = k_d K$ where K is the [Na(18C6)]$^+$ stability constant.

The cryptands C211, C221 and C222 show a remarkable degree of selectivity for alkali metal ions which is mainly due to the matching of the ionic radius for the appropriate coordination number of M$^+$, r_M, to the radius of the cryptand cavity estimated from Corey Pauling Koltun models [4] as seen in Table 1. The most stable cryptates are those where the sizes of M$^+$ and the cryptand cavities are most closely matched. Although the cryptate stabilities generally increase with the decrease in solvent solvating power, the selectivity pattern does not change [52,53]. However, as cryptand size and flexibility increases both selectivity and cryptate stability diminish markedly as is seen for C322.

Because M$^+$ is isolated from the solvent in an inclusive cryptate its chemical shift is almost invariant with change in the nature of the solvent while that of solvated M$^+$ has a significant solvent dependence. This was shown to be the case in ^{7}Li

Table 1
Variation of the cryptate stability constant in water at 298.2 K[a] with cavity radius, r_c, and metal ion radius, r_M
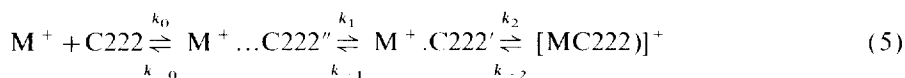
Cryptand	r_c	$\log(K/dm^3 mol^{-1})$[a]					
		$M^+ =$ $r_M^b =$	Li$^-$ 76 pm	Na$^+$ 112 pm	K$^+$ 151 pm	Rb$^+$ 161 pm	Cs$^-$ 174 pm
C211	80 pm		5.5	3.2	<2	<2	<2
C221	110 pm		2.50	5.40	3.95	2.55	<2
C222	140 pm		<2	3.9	5.4	4.35	<2
C322	180 pm		<2	1.65	2.2	2.05	2.0

[a] Ref. [4]. The r_c are estimated from Corey–Pauling–Koltun models.
[b] Ref. [35]. Six- and seven-coordinate r_M are given for Li$^+$ and Na$^+$, respectively. Eight-coordinate r_M are given for K$^+$, Rb$^+$ and Cs$^-$.

NMR studies of $[Li(C211)]^+$ in a range of solvents consistent with $[Li(C211)]^+$ retaining its inclusive structure in solution [54]. In contrast, the ^{23}Na shift of $[Na(C211)]^+$ is sensitive to the nature of the solvent consistent with its exclusive structure in solution [55]. For $[Cs(C222)]^-$, ^{133}Cs NMR studies show that an equilibrium between inclusive and exclusive forms of the cryptate exists in solution while $[Cs(C211)]^+$ and $[Cs(C221)]^-$ exist in the exclusive form only [56–58]. The free cryptand may exist in three major conformations in solution, exo–exo, exo–endo and endo–endo where exo and endo indicate that the nitrogen lone electron pair points outwards from and inwards to the cryptand centre, respectively. In the crystalline state the endo–endo conformation is adopted in cryptates [40–43,59–61] and this appears to be the case in solution also. However, acoustic studies are consistent with a facile solvent dependent equilibrium existing between all three conformations for C222 in several solvents [62,63].

Acoustic studies of $[M(C222)]^+$, where M^+ is Na$^+$, K$^+$, Rb$^+$ and Cs$^+$, in propylene carbonate are in accord with the rate processes

$$M^+ + C222 \underset{k_{-0}}{\overset{k_0}{\rightleftharpoons}} M^+ \ldots C222'' \underset{k_{-1}}{\overset{k_1}{\rightleftharpoons}} M^+.C222' \underset{k_{-2}}{\overset{k_2}{\rightleftharpoons}} [MC222)]^+ \qquad (5)$$

where k_0/k_{-0} characterises the close to diffusion controlled formation of the encounter complex $M^-\ldots C222''$ in the exo–exo form, exclusive $M^+.C222'$ is in the exo–endo form and inclusive $[M(C222)]^+$ is in the endo–endo form [64]. (When $M^+ = K^+$ and Rb$^+$, $10^{-8}k_1 = 7.2$ and $6.0 \, s^{-1}$, and $10^{-7}k_2 = 11$ and $7.6 \, s^{-1}$, respectively, at 298.2 K.) These processes encompass a considerable number of rapid desolvation and conformational changes in the formation of $[M(C222)]^+$ and similar processes also occur in other cryptate systems.

The majority of kinetic studies have been carried out using the slower stopped-flow [65] and NMR methods [66–68] such that the decomplexation (k_d) and complexation (k_c) rate constants represent the slowest steps in a multistep process.

$$M^+ + cryptand \underset{k_d}{\overset{k_c}{\rightleftharpoons}} [M(cryptand)]^+ \qquad (6)$$

Nevertheless, such studies in combination with stability studies yield valuable insight into cryptate complexation processes. Thus, the general decrease in stability of $[M(C221)]^+$ and $[M(C222)]^+$ as the donor power of the solvent increases, as indicated by the Gutmann donor number (D_N) [69–71], is mainly the result of a substantial decrease in k_d while k_c shows a relatively small variation with the nature of the solvent [65,67]. This is consistent with the transition state for the rate determining decomplexation step more closely resembling solvated M^+ and C221 or C222, than either $[M(C221)]^+$ or $[M(C222)]^+$, respectively [65].

Within this extensive span of coronate and cryptate chemistry we have studied the complexation of metal ions by diaza bibracchial lariat ethers, cryptands and modified cryptands as is discussed below.

3. Bibracchial lariat ether complexes

The lariat ethers are either coronands or azacoronands with pendant arms attached to one or more ring carbons or ring nitrogens, respectively [30,72]. The diaza bibracchial lariat ethers 7,13-bis(2-hydroxyethyl)-1,4,10,-trioxa-7,13-diaza-cyclopentadecane (bheC21) and its 2-methoxyethyl analogue (bmeC21), and 7,16-bis(2-hydroxyethyl)-1,4,10,13-tetraoxa-7,16-diazacyclooctadecane (bheC22) and its 2-methoxyethyl analogue (bmeC22) [38,73] occupy a structural niche between the diazacoronands 1,4,10,-trioxa-7,13-diazacyclopentadecane (C21) and 1,4,10,13-tetraoxa-7,16-diazacyclooctadecane (C22) (Fig. 2) and the cryptands C221
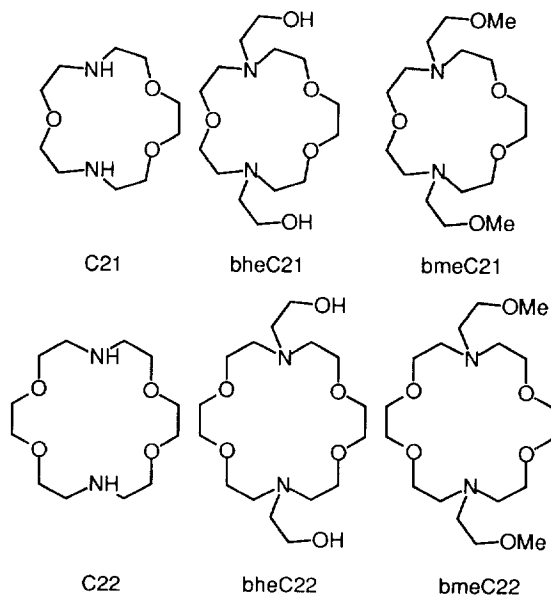

Fig. 2. Schematic representations of some diaza coronands and bibracchial lariat ethers.

and C222 (Fig. 1). In the crystalline state [Na(bheC22)]⁻, [K(bheC22)]⁻ and [Na(bmeC22)]⁺ adopt a *syn* configuration where both arms are on the same side of the macrocyclic ring with eight-coordinate Na⁻ and K⁺ at the centre of a cryptand-like cavity, while [K(bmeC22)]⁺ adopts an *anti* configuration with an arm on either side of the macrocyclic ring coordinated to eight-coordinate K⁺ at its centre [38,73]. This difference is attributed to the greater steric crowding caused by the methyl groups in K(bmeC22)]⁺, but packing forces may also contribute to this departure from the *syn* configuration. Similar structural data is not available for the analogous [M(bheC21)]⁺ and [M(bmeC21)]⁺ species. However, as our X-ray structure of [K(C21)]⁻ shows K⁺ to be 141 pm out of the plane of puckered C21 [74] and Na⁺ is substantially out of the mean plane of [Na(15C5)]⁺ [39], the entry of Na⁺ and K⁻ into the macrocyclic hole appears less likely in [M(bheC21)]⁻ and [M(bmeC21)]⁺. This likelihood diminishes further for all four bibracchial lariat ethers for Rb⁻ and Cs⁺ which are included in the solution studies discussed below [75–77].

The stability constants for the four bibracchial ether complexes of the alkali metal ions and Ag⁺ together with those for C21, C22 [48,78], C221 and C222 [52,53], in several solvents are collected in Table 2. For the alkali metal complexes the general decrease in stability as solvent D_N increases is a result of increasing competition from the solvent for M⁺. In a given solvent the increase in stability: [M(C21)]⁺ < [M(bheC21)]⁺ ∼ [M(bmeC21)]⁻ < [M(C221)]⁺, where the ligands incorporate the fifteen-membered diaza coronand ring, is a consequence of the increasing number of oxygen donor atoms and the "cryptate effect" [4], as is the analogous variation [M(C22)]⁻ < [M(bheC22)]⁺ ∼ [M(bmeC22)]⁺ < [M(C222)]⁺ where the ligands incorporate the eighteen-membered diaza coronand ring. In propylene carbonate C21 and C22 are selective for Na⁺ and K⁺, respectively, while in acetonitrile the stability of [Li(C22)]⁺ approaches that of [Na(C22)]⁺ which is slightly greater than that of [K(C22)]⁺. This demonstrates the influence of changes in solvation on selectivity in these systems. Our [M(bmeC21)]⁺ and [M(bheC21)]⁻, and [M(bmeC22)]⁺ data show changes in selectivity from Li⁺ to Na⁺, and from Na⁺ to K⁻ as the solvent D_N increases. In contrast to the more flexible bibracchial crown ethers, the C221 and C222 cryptands remain selective for Na⁺ and K⁺, respectively, in a similar range of solvents and demonstrate the dominance of the M⁺ size match to that of the cavity over solvation effects in determining selectivity.

While complexes of soft acid Ag⁺ (r_M = 109, 115, 122 and 128 pm for 5, 6, 7 and 8-coordination [35]) are much more stable than their hard acid alkali metal analogues because of a stronger interaction with the diaza donor atoms [79,80], there remains some size selectivity in the bibracchial lariat ether complexes. Thus, [Ag(bheC21)]⁺ and [Ag(bmeC21)]⁻ are slightly more stable than [Ag(bheC22)]⁺ and [Ag(bmeC22)]⁺, and [Ag(C221)]⁺ is slightly more stable than [Ag(C222)]⁺ probably because seven-coordinate Ag⁺ best matches the cavity sizes of the smaller of each ligand pair. A substantial solvent dependence of complex stability also exists with nitrogen donor acetonitrile competing most strongly with the macrocyclic ligands for Ag⁺. In water log(K/dm³ mol⁻¹) for Mg²⁺, Ca²⁺, Sr²⁺ and Ba²⁺ in

Table 2
The variation of complex stability in several solvents at 298.2 K

Complex	Solvent	D_N	$\log(K/\mathrm{dm^3\,mol^{-1}})$ $M^+ =$					
			Li$^+$	Na$^+$	K$^+$	Rb$^+$	Cs$^+$	Ag$^+$
[M(C21)]$^{a+}$	Propylene carbonate	15.1[b]	4.12	4.83	2.25			
[M(C22)]$^{c+}$	Acetonitrile	14.1[b]	4.39	4.45	4.32	3.37	2.26	7.94
[M(C22)]$^{a+}$	Propylene carbonate	15.1[b]	3.59	4.31	4.43	2.93	1.95	15.57
[M(C22)]$^{c+}$	Methanol	19.0[b] 23.5[d]	1.07	1.0	2.04	1.2		9.99
[M(bmeC21)]$^{e+}$	Acetonitrile	14.1[b]	9.13	8.17	5.24	4.39	3.77	7.08
[M(bmeC21)]$^{e+}$	Propylene carbonate	15.1[b]	7.0	7.1	5.0	4.2	3.6	12.2
[M(bmeC21)]$^{e+}$	Methanol	19.0[b] 23.5[d]	3.01	4.89	4.69	3.97	3.46	9.86
[M(bmeC21)]$^{e+}$	Dimethylformamide	26.6[b]	2.23	3.50	3.31	2.84	2.31	8.37
[M(bmeC21)]$^{e+}$	Water	18.1[b] 33.0[d]	<2	<2	<2	<2	<2	7.57
[M(bmeC22)]$^{f+}$	Acetonitrile	14.1[b]	5.80	7.91	6.19	5.24	4.41	6.90
[M(bmeC22)]$^{f+}$	Propylene carbonate	15.1[b]	5.1	6.8	6.0	4.7	4.0	11.7
[M(bmeC22)]$^{f+}$	Methanol	19.0[b] 23.5[d]	2.47	4.57	5.30	4.44	3.66	9.39
[M(bmeC22)]$^{f+}$	Dimethylformamide	26.6[b]	1.93	3.31	3.82	3.08	2.38	8.28
[M(bmeC22)]$^{f+}$	Water	18.1[b] 33.0[d]	<2	<2	2.2	<2	<2	7.10
[M(bheC21)]$^{g+}$	Acetonitrile	14.1[c]	8.61	7.00				6.24
[M(bheC21)]$^{g+}$	Methanol	19.0[b] 23.5[d]	2.85	4.71				9.36
[M(bheC21)]$^{g+}$	Dimethylformamide	26.6[b]	2.36	3.93	3.08	2.50	2.11	9.34
[M(bheC22)]$^{g+}$	Dimethylformamide	26.6[b]	2.29	3.65	4.66	3.56	3.36	9.13
[M(C221)]$^{h+}$	Acetonitrile	14.1[c]	10.33	>11.3	9.5	7.27	5.15	11.24
[M(C221)]$^{h+}$	Propylene carbonate	15.1[c]	9.60	12.09	9.88	7.03	4.92	18.50
[M(C221)]$^{i+}$	Methanol	19.0[b] 23.5[d]	5.38	9.65	8.54	6.74	4.33	14.64
[M(C221)]$^{h+}$	Dimethylformamide	26.6[c]	3.58	7.93	6.66	5.35	3.61	12.41
[M(C222)]$^{h+}$	Acetonitrile	14.1[c]	6.97	9.63	11.3	9.50	4.57	8.99
[M(C222)]$^{h+}$	Propylene carbonate	15.1[c]	6.94	10.54	11.19	9.02	4.1	16.29
[M(C222)]$^{i+}$	Methanol	19.0[b] 23.5[d]	2.6	7.98	10.4	8.98	4.4	12.20
[M(C222)]$^{h+}$	Dimethylformamide	26.6[c]		6.17	7.98	6.78	2.16	10.07

[a] Ref. [48].

[b] Ref. [69].

[c] Ref. [78].

[d] Refs. [70,71].
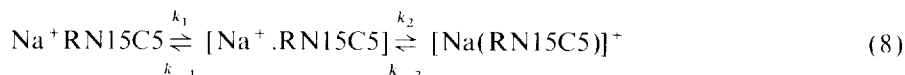
[e] Ref. [76].

[f] Ref. [77].

[g] Ref. [75].

[h] Ref. [53].

[i] Ref. [52].

$[M(bheC21)]^{2-} = \sim 2$, 4.86, 4.15 and 3.99, in $[M(bmeC21)]^{2+} = <2$, 2.8, 3.62 and 3.45, in $[M(bheC22)]^{2+} = <2$, 4.08, 4.29 and 5.33, and in $[M(bmeC22)]^{2+} = <2$, 2.4, 3.64 and 4.36 [81]. Thus, the most stable complexes are $[Sr(bheC21)]^{2+}$ and $[Sr(bmeC21)]^{2+}$ ($r_M = 121$ pm for 7-coordinate Sr^{2+}) and $[Ba(bheC22)]^{2+}$ and $[Ba(bmeC22)]^{2+}$ ($r_M = 142$ pm for 8-coordinate Ba^{2+}), consistent with cavity size being a significant factor in determining complex stability. The border-line hard acid divalent first row transition metal ions form similar complexes of increased stability probably because they coordinate nitrogen more strongly than the hard acid alkaline earth ions.

Our ^7Li and ^{23}Na NMR kinetic studies of the monomolecular M^+ exchange on the bibracchial lariat ether $[ML]^+$ complexes

$$M^+ + L \underset{k_d}{\overset{k_c}{\rightleftharpoons}} [ML]^+ \tag{7}$$

show that the greater decomplexation rate (k_d) of the bibracchial lariat ether complexes is largely the cause of their lower stabilities ($K = k_c/k_d$) by comparison with those of the corresponding and less flexible cryptates [82] (Table 3). For each complex, k_c and k_d characterise the slowest of the sequential steps in either direction. While k_d are similar for the Li^+ and Na^+ bibracchial lariat ethers, the $\Delta H_d^{\ddagger}$ for the former species are smaller but this is compensated for by their more negative $\Delta S_d^{\ddagger}$.

The faster acoustic method has detected two of the Na^+ complexation sequence steps in the formation of $[Na(RN15C5)]^+$

$$Na^+RN15C5 \underset{k_{-1}}{\overset{k_1}{\rightleftharpoons}} [Na^+.RN15C5] \underset{k_{-2}}{\overset{k_2}{\rightleftharpoons}} [Na(RN15C5)]^+ \tag{8}$$

where RN15C5 is the single arm lariat ether, 1-methoxyethoxyethyl-1,4,7,10,13-tetraoxa-1-azacyclopentadecane [83]. The ($k_1/k_{-1} = K_1$) step is the initial complexation, where Na^+ remains outside the coronand ring, and the second (k_2/k_{-2}) step results in Na^+ being coordinated within the

Table 3
Parameters for Li^+ and Na^+ exchange in several complexes in methanol

Complex	$10^{-5}k_c(298.2 \text{ K})$ (dm^3 mol^{-1} s^{-1})	$k_d(298.2 \text{ K})$ (s^{-1})	$\Delta H_d^{\ddagger}$ (kJ mol^{-1})	$\Delta S_d^{\ddagger}$ (J K^{-1} mol^{-1})
[Li(bheC21)][a]	43	6070	27.1	−81.5
[Li(bmeC21)][b]	20.2	1970	20.4	−113
[Li(C221)][c]	192	78.4	23.8	−129
[Na(bheC22)][a]	3058	4130	42.8	−32.0
[Na(bmeC22)][d]	903	2430	59.9	20.8
[Na(C222)][e]	2700	2.87		

[a] Ref. [75].
[b] Ref. [76].
[c] Ref. [82].
[d] Ref. [77].
[e] Ref. [65].

coronand ring and by the methoxyethoxyethyl arm with $k_1 = 9.0 \times 10^{10}$ dm^3 mol^{-1} s^{-1}, $k_{-1} = 2.1 \times 10^8$ s^{-1}, $K_1 = 429$ dm^3 mol^{-1}, $k_2 = 1.2 \times 10^7$ s^{-1}, $k_{-2} = 1.5 \times 10^5$ s^{-1} and $K_2 = 80$ at 298.2 K. When R is replaced by CH$_3$ the corresponding data is $k_1 = 9.1 \times 10^9$ dm^3 mol^{-1} s^{-1}, $k_{-1} = 5.9 \times 10^7$ s^{-1}, $K_1 = 154$ dm^3 mol^{-1}, $k_2 = 5.9 \times 10^6$ s^{-1}, $k_{-2} = 3.9 \times 10^5$ s^{-1} and $K_2 = 14.9$ dm^3 mol^{-1}, which demonstrates the complex stabilising effect of the methoxyethoxyethyl arm.

4. Modified cryptates

The series 4,7,13,16-tetraoxa-1,10-diazabicyclo[8.8.2]eicosane (C22C$_2$), its -[8.8.5]tricosane (C22C$_5$) and -[8.8.8]hexacosane (C22C$_8$) analogues, and 4,7,13-trioxa-1,10-diazabicyclo[8.5.5]eicosane (C21C$_5$) shown in Fig. 3, may be viewed as diazacoronands in which the two amine hydrogens have been substituted by a -(CH$_2$)$_n$- bridge, where $n = 2$, 5 and 8, and are related to the cryptands where this bridge is replaced by -(CH$_2$)$_2$O((CH$_2$)$_2$O)$_x$(CH$_2$)$_2$-. Because of this relationship and their macrobicyclic nature, the members of this series are conveniently referred to as modified cryptands and provide an opportunity to study the influence of a preformed cavity on selectivity when one arm is devoid of coordinating groups.

Unlike the cryptands, the smallest member of the series. C22C$_2$, has a clam-like structure where the upper and lower -(CH$_2$)$_2$O(CH$_2$)$_2$O(CH$_2$)$_2$- jaws are hinged about the >N(CH$_2$)$_2$N< moiety [84 88]. (The generic name, diptychand, derived from ditypchos and meaning hinged double tablet has been proposed for C22C$_2$ [84].) The dihedral angle between the mean planes delineated by the two hinge nitrogens and the pairs of oxygens in each jaw is calculated [89] as 88.4, 70.9, 89.6 and 100 from the crystal structures of C22C$_2$, [Li(C22C$_2$)]$^+$, [Na(C22C$_2$)]$^+$ and [K(C22C$_2$)]$^+$, respectively [84–88]. This variation of jaw angle presents the potential for a different mode of selectivity for metal ions by comparison with that of the less flexible cryptands discussed earlier in which metal ion selectivity is predominantly determined by the fit of the metal ions to the cryptand cavities.

In acetonitrile, $\log(K/\text{dm}^3 \text{ mol}^{-1})$ for [M(C22C$_2$)]$^+$ varies in the sequence 7.8, 9.4, 7.2, 5.0, 9.4 and 10.4 when M$^+$ = Li$^+$, Na$^+$, K$^+$, Cs$^+$, Ag$^+$ and Tl$^+$, respectively, and the analogous values in dimethylformamide are 3.5, 6.1, 3.2, 2.7, 9.4 and
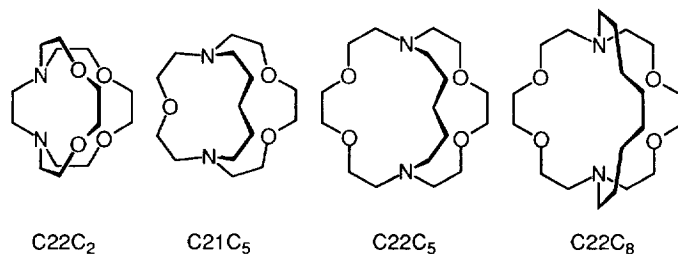

Fig. 3. Schematic representations of some modified cryptands.

6.7 [89,90]. For the alkali metal ion $[M(C22C_2)]^+$ there is a decrease in stability on going from acetonitrile to dimethylformamide as the solvent D_N increases, but the most stable complex in both solvents is $[Na(C22C_2)]^+$ consistent with there being the least strain in its structure where the coordinated $C22C_2$ jaw angle is close to that observed in free $C22C_2$. In $[Li(C22C_2)]^+$ the jaw angle is less than that in free $C22C_2$ while in $[K(C22C_2)]^+$ the jaw angle is greater, and in both cases it appears that this results in structural strain which diminishes stability. ^{7}Li and ^{23}Na NMR studies yield $10^{-5}k_c(298.2\ K) = 7.60$ and $155\ dm^3\ mol^{-1}\ s^{-1}$, $k_d(298.2\ K) = 240$ and $12.3\ s^{-1}$, $\Delta H_d^{\ddagger} = 22.5$ and $64.0\ kJ\ mol^{-1}$, and $\Delta S_d^{\ddagger} = -124$ and $-9.5\ J\ K^{-1}\ mol^{-1}$ for monomolecular metal ion exchange in $[Li(C22C_2)]^+$ and $[Na(C22C_2)]^+$, respectively, in dimethylformamide [89,90]. Thus, the greater stability of $[Na(C22C_2)]^+$ arises from its greater k_c and smaller k_d, by comparison with those of $[Li(C22C_2)]^+$. The larger k_d for $[Li(C22C_2)]^+$ arises from a smaller $\Delta H_d^{\ddagger}$ and more negative $\Delta S_d^{\ddagger}$ which probably reflect the release of greater structural strain and significantly greater resolvation of Li^- in the transition state than is the case for $[Na(C22C_2)]^+$ in which structural strain is less and Na^- is more exposed to solvent in the ground state so that less resolvation occurs in the transition state.

In dimethylformamide $[Na(C22C_2)]^+$ is less stable than its Ag^- and Tl^+ analogues because this hard base oxygen donor solvent competes more effectively with $C22C_2$ for hard acid Na^+ than it does for soft acid Ag^- and Tl^+ which show a greater tendency to coordinate soft base nitrogen atoms [79,80]. This effect superimposes on the effects of cation size. In the soft base nitrogen donor acetonitrile this competition changes so that $[Na(C22C_2)]^+$ stability increases substantially while that of $[Ag(C22C_2)]^+$ is unchanged. In dimethylformamide, the greater stability of $[Ag(C22C_2)]^+$ by comparison with that of $[Tl(C22C_2)]^+$ mainly reflects the greater size of Tl^- $(r_M = 150\ pm)$ and the greater strain in $[Tl(C22C_2)]^+$. However, $[Tl(C22C_2)]^+$ becomes more stable than $[Ag(C22C_2)]^+$ in acetonitrile probably because the acid character of Tl^+ lies in between those of Ag^+ and hard acid K^+ [91,92] and acetonitrile competes more effectively for Ag^+ than for Tl^-.

The modified cryptand, $C21C_5$, is directly comparable to $C211$ and our crystal structures of $[Na(C211)]SCN$ and $[Na(C21C_5)]SCN$ [93] show both to form exclusive cryptates with Na^+ positioned on a 15-membered trioxa diaza cryptand face with a SCN^- within bonding distance. In $[Na(C21C_5)]SCN$, Na^- is 37 pm distant from the trioxa plane, while in $[Na(C211)]SCN$ Na^+ is 14 pm from the trioxa plane and the decreased distance is attributable to the Na^- interaction with the fourth $C211$ oxygen which is 266.2 pm distant. Reflecting the smaller size of Li^-, there is no bonding interaction between Li^- and SCN^- in the inclusive $[Li(C21C_5)]SCN$ cryptate [94] as is also the case for inclusive $[Li(C211)]SCN$ [40].

The presence of the fourth oxygen in $[Li(C211)]^+$ and $[Na(C211)]^+$ causes them to be considerably more stable than $[Li(C21C_5)]^+$ and $[Na(C21C_5)]^+$, respectively, in dimethylformamide and other solvents as a consequence of the greater electrostatic interaction of $C211$ with Li^+ and Na^- than is the case for $C21C_5$ [55,67,95–100] (Table 4). While inclusive $[Li(C211)]^-$ is more stable than exclusive $[Na(C211)]^-$, exclusive $[Na(C21C_5)]^+$ is more stable than $[Li(C21C_5)]^+$ which, from ^{7}Li chemical shift measurements, appears to exist in an equilibrium between exclusive and inclusive

Table 4
Parameters for $[Li(C21C_5)]^+$, $[Li(C211)]^+$, $[Na(C21C_5)]^+$ and $[Na(C211)]^+$ in several solvents

Solvent	D_N	$10^{-5}k_c$ (dm³ mol⁻¹ s⁻¹)	k_d (s⁻¹)	$\Delta H_d^‡$ (kJ mol⁻¹)	$\Delta S_d^‡$ (J K⁻¹ mol⁻¹)	log (K/dm³ mol⁻¹)
$[Li(C21C_5)]^+$						
Acetonitrile[a]	14.1[b]					4.15
Methanol[a]	19.0[b] 23.5[c]	0.221	21.6	36.1	−98.4	3.00
Dimethylformamide[a]	26.6[b]	0.073	116	38.4	−76.5	1.80
$[Li(C211)]^+$						
Acetonitrile	14.1[h]			–		>10[d]
Methanol[e]	19.0[b] 23.5[c]	4.8	0.0044			8.04
Dimethylformamide[f]	26.6[b]	1.27	0.013	64.4	−64.8	6.99[d]
$[Na(C21C_5)]^+$						
Acetonitrile[g]	14.1[b]	100	84.8	57.9	−13.8	5.08[h]
Propylene carbonate[g]	15.1[b]	25.5	19.4	70.3	15.3	5.12[b]
Acetone[g]	17.0[b]	84	878	54.4	−6.1	3.98[h]
Methanol[g]	19.0[b] 23.5[c]	104	1800	44.9	−31.9	3.76[h]
Dimethylformamide[g]	26.6[b]	214	28800	40.0	−25.3	2.87[h]
Pyridine[g]	33.1[b]	4.9	93.5	62.8	3.3	3.72[h]
$[Na(C211)]^+$						
Propylene carbonate[i]	15.1[b]	210	0.036			8.76[d]
Water[i]	18.1[b] 33.0[c]	0.754	47.6	67.2	12.6	3.2[d]
Methanol[e]	19.0[b] 23.5[c]	31.0	2.5	–		6.1[d]
Trimethylphosphate[k]	23.0[b]	16.6	6.92	62.2	−20.3	5.38
Triethylphosphate[l]	26.0[m]	4.3	8.2	67.0	−2.6	4.72
Tri-n-butylphosphate[l]	23.7[b]	3.1	3.6	84.7	50.5	4.94
Dimethylformamide[l]	26.6[b]	19.2	12.1	83.5	55.9	5.23[d]
Dimethylacetamide[n]	27.8[b]	24.9	45.2	64.8	4.3	4.74
Diethylformamide[n]	30.9[b]	22.9	18.2	67.1	4.4	5.10
Dimethyl sulfoxide[i]	29.8[b]	14.5	34.0	69.5	17.4	4.63[d]

[a] Ref. [95].
[b] Ref. [69].
[c] Refs. [70,71].
[d] Ref. [53].
[e] Ref. [52].
[f] Ref. [66].
[g] Ref. [67].
[h] Ref. [96].
[i] B.G. Cox, J. Garcia-Rosas and H. Schneider, J. Phys. Chem., 84 (1980) 3178.
[j] Ref. [55].
[k] Ref. [97].
[l] Ref. [98].
[m] Y. Marcus, J. Soln. Chem., 13 (1984) 599.
[n] Ref. [97].

forms in solution [95]. Thus, the lower stability of $[Li(C21C_5)]^+$ is probably a consequence of the greater solvation energy of Li^+ by comparison with that of Na^+. The greater stability of $[Li(C211)]^+$ is mainly due to its much lower decomplexation rate (k_d) by comparison with that of $[Na(C211)]^+$, while the greater complexation rate of $[Na(C21C_5)]^+$ (k_c) causes it to be more stable than $[Li(C21C_5)]^+$.

It was noted in Section 2 that the decrease in stability of alkali metal $[M(C221)]^+$ and $[M(C222)]^+$ with increase in solvent D_N was largely because k_d showed major increases while the changes in k_c were relatively small [65]. A similar effect is seen for $[Na(C21C_5)]^+$ (Table 4) and may be interpreted in terms of the simplified reaction profile shown in Fig. 4, which refers only to the slowest complexation and decomplexation steps of a multistep process [67]. Thus, $\Delta G_c^{\ddagger}$ is set constant to reflect its relatively small variation with solvent by comparison with that of $\Delta G_d^{\ddagger}$. Because $\Delta G_d^{\ddagger}$ is the difference between $\Delta G_r^{\ddagger}$ and $\Delta G_s^{\ddagger}$, and ΔG^0 is the difference between $\Delta G_d^{\ddagger}$ and $\Delta G_c^{\ddagger}$, both $\Delta G_d^{\ddagger}$ and ΔG^0 are decreased by a strong donor solvent because $\Delta G_s^{\ddagger}$ is large and vice-versa for a weak donor solvent. (The deviation from this pattern in pyridine may arise because its nitrogen donor atom is embedded in the aromatic ring and the resulting steric hindrance renders it less able to compete for Na^+ than is the case for the smaller solvent molecules.) This effect is also discernible for $[Na(C211)]^+$ in propylene carbonate, methanol and dimethylformamide. However, as solvent molecular size increases steric effects on solvation may cause deviations from the simple model proposed above.

The crystal structures of $[M(C22C_5)]^+$ show a trend where Na^+ lies within the mean plane of the four cryptand oxygens while K^+ is 36.9 and 44.1 pm (there are two $[K(C22C_5)]^+$ species in the crystal) and Cs^+ is 129.96 pm above this mean plane [101,102]. While the four oxygens of $[Na(C22C_5)]^+$ are almost perfectly coplanar, deviation from coplanarity increases progressively in the K^+ and Cs^+

ΔG^0 = free energy of complexation
$\Delta G_c^{\ddagger}$ = activation free energy of complexation
$\Delta G_d^{\ddagger}$ = activation free energy of decomplexation
$\Delta G_r^{\ddagger}$ = structural rearrangement component of $\Delta G_d^{\ddagger}$
$\Delta G_s^{\ddagger}$ = solvation component of $\Delta G_d^{\ddagger}$
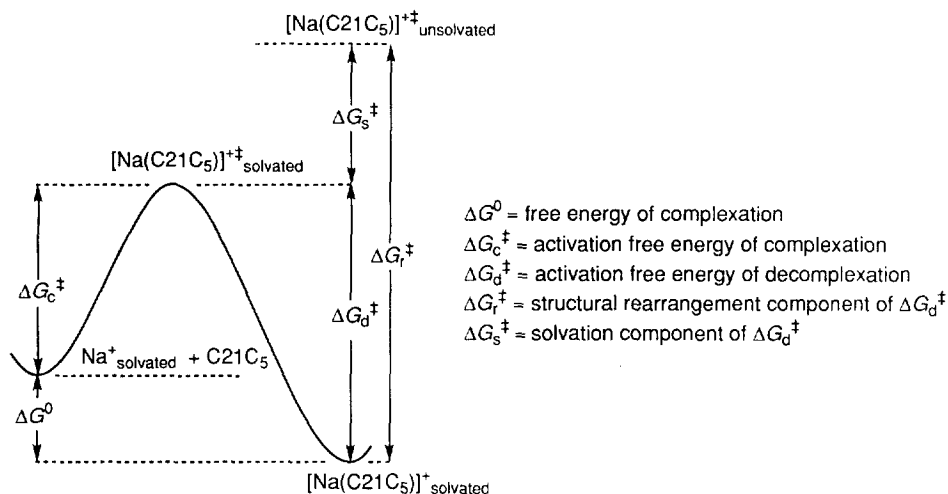
Fig. 4. Free energy profile for $[Na(C21C_5)]^+$.

analogues, and in none of these cryptates are the cryptand nitrogens in bonding distance of the alkali metal ion. Comparison with inclusive $[Na(C221)]^+$ and exclusive $[K(C221)]^+$ discussed earlier [41], shows that the absence of a fifth oxygen in $[Na(C22C_5)]^+$ causes Na^+ to interact preferentially with the four oxygens in the face of the cryptand and to become distant from the two nitrogens, and that the size of K^- excludes it from coplanarity with the four oxygens of $[K(C22C_5)]^+$ as it does in $[K(C221)]^+$. (An unusual feature of $C22C_5.H_3O.ClO_4$ is the position of the H_3O^+ oxygen 66.6 pm above the plane of the four cryptand oxygens [102].)

The alkali metal $[M(C22C_5)]^+$ show a variation in M^+ selectivity and are of lower stability than $[M(C221)]^+$ which is selective for Na^- [102,103] (Table 5). These differences are attributable to the greater electrostatic attraction between M^+ and C221 in $[M(C221)]^+$ and the inclusive nature of $[Na(C221)]^+$. The weaker interactions in $[M(C22C_5)]^+$ result in lower stabilities and in solvation of M^+ being more influential in determining selectivity. A similar relationship holds for $[M(C222)]^+$ and $[M(C22C_8)]^-$ [104]. All four of the above cryptands may be viewed as derivatives of monocyclic C22, and $[M(C221)]^+$, $[M(C22C_5)]^+$ and $[M(C222)]^+$ are more stable than $[M(C22)]^-$ [105–107] (Table 5). This is unsurprising for $[M(C221)]^-$ and $[M(C222)]^+$ because of their extra oxygen donor atoms and the cryptate effect [4,5]. The enhanced stability of $[M(C22C_5)]^+$ is probably a consequence of the C_5 arm restricting conformational flexibility of the 18-membered ring and blocking solvent access to M^+ on one side of $[M(C22C_5)]^+$. (Some support for this is adduced from the solid state where K^- lies in the plane of the four oxygens of $[K(C22)]^+$ [108] while it lies above this plane in $[K(C22C_5)]^+$ [102].) However, the stability of $[M(C22C_8)]^+$ is lower than that of $[M(C22C_5)]^+$ and approaches that of $[M(C22)]^+$ presumably because of the greater flexibility of the C_8 arm [104]. The stabilities of the cryptates formed by $C21C_5$, $C22C_2$, $C22C_5$ and $C22C_8$ with bivalent metal ions largely reflect the influence of the same structural factors observed for their alkali metal analogues [109,110].

5. Metal complexes of pendant arm macrocyclic ligands

Since the synthesis of 1,4,7,10-tetraazacyclododecane (cyclen) [20] and 1,4,8,11-tetraazacyclotetradecane (cyclam) [21] and ligands derived from them (Fig. 5) a field of complexation research encompassing a wide range of metal ions has evolved [22,28,29,31,111]. We are particularly interested in the metal complexes of the cyclen and cyclam derivatives where a coordinating pendant arm is attached to each nitrogen of the macrocyclic ring [24,26,27,112–120] (Fig. 5). Within this area our studies have been mainly concerned with the interplay between stability, lability and structure in complexes of mono- and bivalent metal ions, and this is reflected in the discussion which follows. Comparisons are made with the fascinating chemistry of closely related trivalent lanthanide complexes.

The first alkali metal complexes of pendant arm macrocyclic ligands to be the subject of quantitative stability and kinetic studies were those of 1,4,7,10-tetrakis(2-hydroxyethyl)-1,4,7,10-tetraazacyclododecane (thec12) and its

Table 5
Stability constants for some alkali metal complexes

| Solvent | $\log(K/dm^3\ mol^{-1})$ | | | | |
| | $M^+ =$ | | | | |
	Li^+	Na^+	K^+	Rb^+	Cs^+
$[M(C22C_5)]^+$					
Acetonitrile[a,b]	6.07	7.55	6.26	5.5	4.57
Propylene carbonate[a]	5.36	5.95	7.56	6.66	5.16
Methanol[b]	2.30	5.41	5.8	5.7	4.8
Dimethylformamide[b]	2.21	3.66	3.85	3.82	2.90
$[M(C221)]^+$					
Acetonitrile[c]	10.33	>11.3	9.5	7.27	5.15
Propylene carbonate[c]	9.60	12.09	9.88	7.03	4.92
Methanol[d]	5.38	9.65	8.54	6.74	4.33
Dimethylformamide[c]	3.58	7.93	6.66	5.35	3.61
$[M(C22C_8)]^+$					
Acetonitrile[c]	3.7	4.86	5.09	3.85	3.13
Dimethylformamide[c]	1.9	2.3	2.6	2.2	2.0
$[M(C222)]^+$					
Acetonitrile[c]	6.97	9.63	11.3	9.50	4.57
Dimethylformamide[c]		6.17	7.98	6.78	2.16
$[M(C22)]^+$					
Acetonitrile	4.39[f]	4.49[g]	4.35[g]	3.37[h]	2.25[g]
		4.30[h]	4.32[h]		2.48[h]

[a] Ref. [102].
[b] Ref. [103].
[c] Ref. [53].
[d] Ref. [52].
[e] Ref. [104].
[f] Ref. [105].
[g] Ref. [106].
[h] Ref. [107].
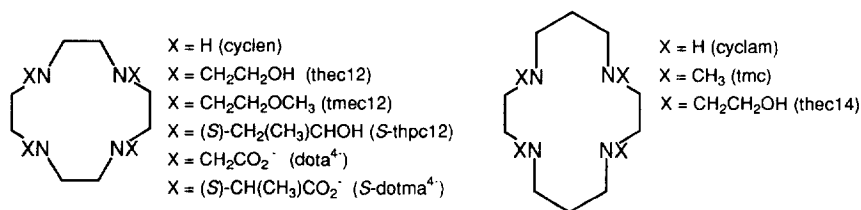
Fig. 5. Schematic representations of some tetraaza-macrocyclic ligands.

2-methoxy (tmec12) and (S)-2-hydroxypropyl (Sthpc12) analogues (Fig. 6 and Fig. 7) [113,116–120]. These three ligands form complexes with all of the alkali metal ions and Ag$^+$, and their stability constants appear in Table 6. It is seen that metal ion selectivity is less than for the cryptates discussed earlier, and that there is a strong dependence of complex stability on the nature of the solvent, and on the ligand. This is consistent with complex stability being dominated by a combination of (i) the solvation energy of the alkali metal ion, (ii) the electron donating power of the solvent as indicated by D_N, (iii) the coordinating power of the ligand donor
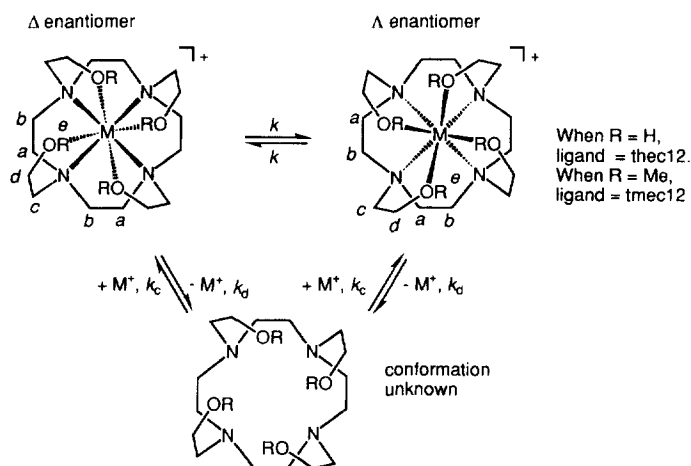
Fig. 6. Enantiomerisation of Δ and Λ[M(thec12)]$^+$ and Δ and Λ[M(tmec12)]$^+$ and M$^+$ exchange in both systems. The Δ and Λ enantiomers are those where the pendant arms assume a clockwise and anticlockwise chirality, respectively, when the structure is viewed from the centre of the four oxygen plane looking towards M$^+$ and the nitrogen plane beyond.
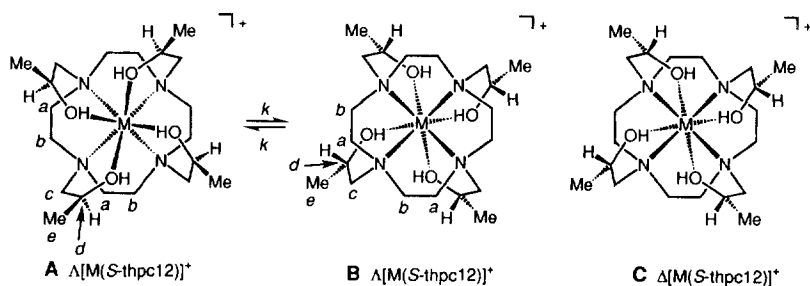
Fig. 7. The exchange process for equivalent forms of the Λ[Na(S-thpc12)]$^+$ diastereomer, A and B, leading to the exchange of the macrocycle carbons between environments a and b. The undetected Δ[Na(S-thpc12)]$^+$ diastereomer is shown as C. The Δ and Λ diastereomers are those where the pendant arms assume a clockwise and anti-clockwise chirality, respectively, when the structure is viewed down the C$_4$ axis from the four oxygen plane looking towards Na$^+$ and the nitrogen plane beyond. The rotation of the plane delineated by the four oxygens away from eclipsing that delineated by the four nitrogens is exaggerated for illustration purposes.

Table 6
Variation of stability of [M(thec12)]$^+$, [M(tmec12)]$^-$ and [M(S-thpc12)]$^-$ with M$^+$ and solvent at 298.2 K and $I = 0.05$ mol dm^{-3} (NEt$_4$ClO$_4$)

| Solvent | $\log(K/\text{dm}^3 \text{mol}^{-1})$ | | | | | |
| | M$^+$ = | | | | | |
	Li$^+$	Na$^+$	K$^+$	Rb$^+$	Cs$^+$	Ag$^+$
[M(thec12)]$^+$ [a]						
Acetonitrile	8.07	6.66	3.40	3.00	2.90	9.35
Propylene carbonate	8.90	7.49	5.91	4.23	4.04	14.00
Methanol	3.09	4.53	2.43	2.20	1.90	12.57
Dimethylformamide	2.99	3.37	1.59	1.39	1.23	11.16
[M(tmec12)]$^+$ [b]						
Acetonitrile	9.34	9.13	6.07	4.85	3.55	12.30
Propylene carbonate	8.0	8.2	6.7	6.2		15.3
Methanol	4.1	6.2	3.9	3.0	2.5	14.2
Dimethylformamide	3.61	5.68	3.62	2.73	2.28	13.73
Water	<2	2.20	<2	<2	<2	12.62
[M(S-thpc12)]$^+$ [c]						
Methanol	4.0	4.8	3.5	3.4	3.2	12.8

[a] Refs. [116,118].

[b] Ref. [119].

[c] Ref. [120].

groups, and (iv) the ability of the ligand to assume a conformation which optimises bonding with M$^+$. Thus, as the solvation energy of M$^+$ increases with D_N the balance among (i)–(iv) changes and the variation of complex stability with the nature of M$^+$ changes. The change from hydroxy to methoxy groups in thec12 and tmec12, respectively, causes a substantial increase in stability attributable to the greater electron donor power of the methoxy groups. Differences in stability between [M(thec12)]$^+$ and [M(S-thpc12)]$^-$ are probably due to a combination of the hydrophobicity and the stereochemical effects of the methyl groups of the latter complex. The stabilities of the Ag$^+$ complexes are substantially greater than their alkali metal analogues because the soft acid nature of Ag$^+$ causes it to coordinate the macrocycle amine groups more strongly. In keeping with this, the Ag$^+$ complex stability is decreased in nitrogen donor acetonitrile.

Both thec12 and tmec12 are achiral and ^{13}C NMR studies are consistent with them forming eight-coordinate Δ and Λ enantiomeric complexes with Li$^+$, Na$^+$ and K$^+$ as shown schematically in Fig. 6. In the solid state, however, [Li(thec12)]$^+$ and its Na$^+$ and K$^+$ analogues are five-, seven- and eight-coordinate, respectively, with all four macrocyclic nitrogens coordinating, but with the coordination of all four hydroxy groups only occurring in [K(thec12)]$^+$ [112,121,122]. Thus, differences in

coordination number in the solution and crystalline states are attributable to packing forces and inter-complex hydrogen bonding in the latter state.

The solution coordination numbers and stereochemistries of $[M(thec12)]^+$ and $[M(tmec12)]^+$ are derived from slow exchange ^{13}C NMR spectra where a single set of resonances for the pendant arms show them to be equivalent while the two resonances arising from the macrocycle ring carbons show them to exist as two inequivalent sets (Fig. 8). As the temperature increases the macrocyclic ring resonances (a and b) coalesce through enantiomerisation while the pendant arm resonances (c and d for $[M(thec12)]^+$, and c, d and e for $[M(tmec12)]^-$) show little variation other than some narrowing and small chemical shift changes associated with decreasing viscosity and changing dielectric constant. This is consistent with exchange occurring between the approximately square antiprismatic Δ and Λ enantiomers of $[M(thec12)]^+$ and $[M(tmec12)]^-$ in which the square planes are delineated by four oxygens and four nitrogens [117 119] (Fig. 6). This enantiomerisation inverts each nitrogen as a consequence of the exchange of the macrocyclic ring carbons between environments a and b.

The introduction of a chiral centre into each pendant arm in 1,4,7,10-tetrakis((S)-2-hydroxypropyl)-1,4,7,10-tetraazacyclododecane (S-thpc12) promises the formation of Δ and $\Lambda[Na(S-thpc12)]^+$ diastereomers on complexation of Na^+ (Fig. 7). Each diastereomer should exhibit a set of five ^{13}C resonances, however, at low temperatures only one such set of resonances is observed consistent with either only the Δ or only the $\Lambda[Na(S-thpc12)]^-$ diastereomer existing at detectable levels, or both diastereomers having very similar chemical shifts [120]. As temperature increases the macrocyclic ring resonances (a and b) coalesce, and minor nonexchange induced changes occur in the pendant arm resonances (c, d and e) in an analogous manner to that seen in Fig. 8, as do the corresponding resonances for the Li^- and K^+ analogues. In a preliminary communication we interpreted this in terms of exchange between Δ and $\Lambda[Na(S-thpc12)]^+$ for which the chemical shifts were very similar [117]. Subsequently, our molecular orbital calculations through Gaussian 94 using the LanL2DZ basis set [123] showed the very much more stable diastereomer to be $\Lambda[Na(S-thpc12)]^+$ which has a distorted cubic structure (twist angle $\phi = 5.3$) delineated by the parallel planes of the four oxygens and the four nitrogens. Thus, it now seems likely that the exchange involves the identical $\Lambda[Na(S-thpc12)]^+$ diastereomers as shown in Fig. 7; an interpretation which also explains the observation of only five ^{13}C resonances at low temperature. (A similar interpretation applies to free ΛS-thpc12 for which $k(298.2 \text{ K}) = 34 800 \text{ s}^{-1}$, $\Delta H^{\ddagger} = 53.9 \text{ kJ mol}^{-1}$ and $\Delta H^{\ddagger} = 22.8 \text{ J K}^{-1} \text{ mol}^{-1}$.) This exchange has no effect on the pendant arm environment, but exchanges the macrocyclic ring carbons between environments a and b. While the sequence of events producing the exchange is unknown, it is clear that each nitrogen has to undergo two inversions, and that a single inversion of all four nitrogens would produce the undetected $\Delta[M(S-thpc12)]^-$ diastereomer. In the crystalline state only the Λ chirality has been found as exemplified by $\Lambda[Pb(S-thpc12)]^{2+}$ [114] and $\Lambda[Bi(S-thpc12)]^{3+}$ [124].

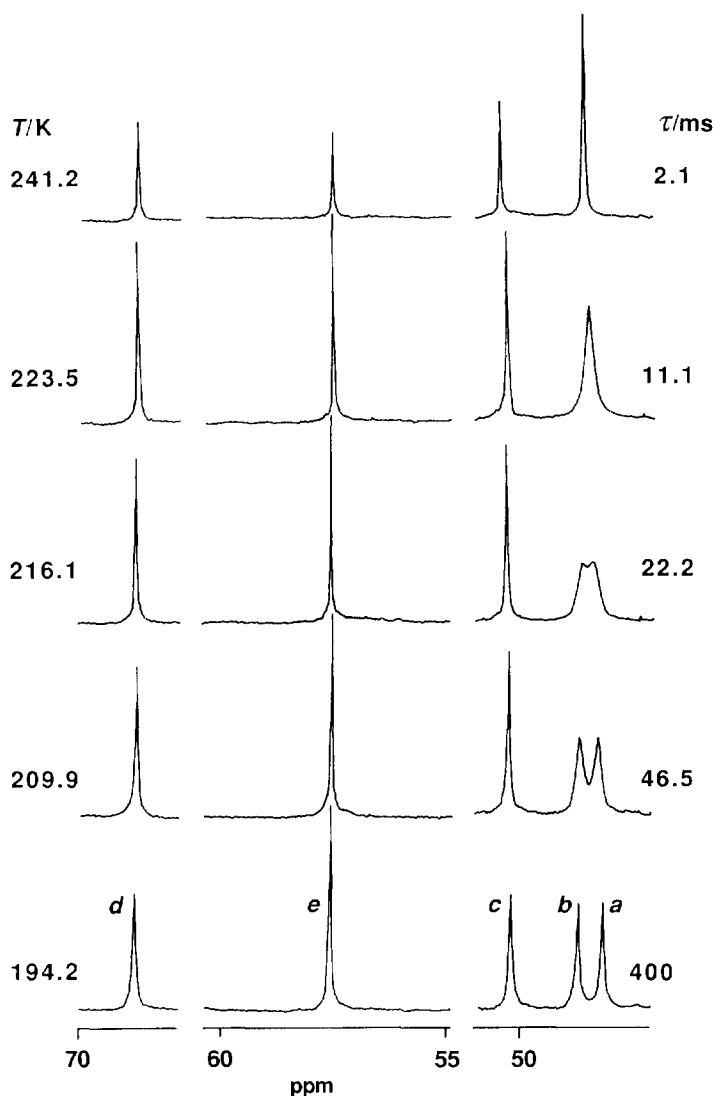The rate parameters for the enantiomerisation of $[M(thec12)]^-$ and

Fig. 8. Exchange modified 75.47 MHz ^{13}C NMR spectra of 0.10 mol dm ^{3} [Li(tmec12)]ClO$_4$ in ^{12}C-enriched [^{2}H$_4$]methanol. Experimental temperatures and derived site lifetimes, τ, appear to the left and and right of the figure (adapted from Ref. [119]).

[M(tmec12)]$^+$, together with those for monomolecular metal ion and ligand exchange, do not show obviously systematic variations (Table 7). This is probably because the contributions to $\Delta G^{\ddagger}$ vary in relative magnitude with M$^+$ and the ligand, and arise from a range of sources which include the metal to ligand bond energies and the magnitude of strain in the ligand. For five of the complexes in Table 7 enantiomerisation is much faster than metal ion and ligand exchange while for

Table 7
Parameters for enantiomerisation, diastereomer exchange, and ligand and metal ion exchange in ^{13}C enriched [^{2}H$_4$]-methanol

Species	Enantiomerisation or diastereomer exchange			Ligand or metal ion exchange			
	k_e(298.2 K) (s^{-1})	$\Delta H^{\ddagger}$ (kJ mol^{-1})	$\Delta S^{\ddagger}$ (J K^{-1} mol^{-1})	k_d(298.2 K) (s^{-1})	$\Delta H_d^{\ddagger}$ (kJ mol^{-1})	$\Delta S_d^{\ddagger}$ (J K^{-1} mol^{-1})	$10^5 k_c$(298.2 K) (dm^3 mol^{-1} s^{-1})
[Li(thec12)]$^-$[a]	18300	41.3	−25.0	424[b]	37.7	−68.2	5.2
[Na(thec12)]$^-$[a]	7100	24.6	−88	729[c]	38.0	−62.8	9.0
				332[b]	65.6	23.3	113
				209[d]	68.3	28.4	71
[K(thec12)]$^-$[a]	7000	53.7	8.7	12300[b]	50.5	2.8	33.1
[Li(tmec12)]$^-$[e]	32800	41.4	−19.7	23.0[b]	46.1	−64	3.0
				18.2[c]	44.8	−70.5	2.3
[Na(tmec12)]$^+$[e]	1470	31.4	−78.8	<14[b]	–	–	–
				≪50[d]			
[K(tmec12)]$^+$[e]	415	50.7	−24.7	34.1[b]	79.9	52.5	2.7
A[Na(S-thpc12)]$^-$[f]	125	26.3	−116	64.3[b]	62.8	0.3	40.6
				49.0[d]	64.9	5.1	30.9

[a] Ref. [118].
[b] Ligand exchange.
[c] Li$^+$ exchange. Ref. [116]
[d] Na$^+$ exchange.
[e] Ref. [119].
[f] Refs. [117,120].

$[K(thec12)]^+$, monomolecular ligand exchange is approximately twice as rapid as enantiomerisation. The double nitrogen inversion of $[Na(S\text{-}thpc12)]^-$ is twice as fast as Na^+ and ligand exchange and exhibits very different activation parameters.

The ^{13}C NMR spectra of the Li^- and Na^+ complexes of the smaller 1,4,7-tris(2-hydroxyethyl)-1,4,7-triazacyclononane (thec9) [125] are consistent with their existence as distorted trigonal prismatic six-coordinate Δ and Λ enantiomers where the two parallel trigonal planes are delineated by three oxygens and three nitrogens, respectively. Molecular orbital calculations show that the trigonal twist angle ϕ for Δ and $\Lambda[Na(thec9)]^+$ is 10.0° which compares with $\phi = 4.5^\circ$ for $[Zn(S\text{-}thpc9)]^{2+}$ in the solid state [126]. ($\phi = 0^\circ$ for trigonal prismatic stereochemistry.) Both Δ and $\Lambda[Li(thec9)]^+$ and their Na^+ analogues enantiomerise more rapidly in methanol than their thec12 analogues as shown by $k = 1.11 \times 10^6$ and $2.27 \times 10^5\,s^{-1}$ at 298.2 K, $\Delta H^\ddagger = 27.2 \pm 0.3$ and $21.7 \pm 0.2\,kJ\,mol^{-1}$, and $\Delta S^\ddagger = -36.3 \pm 1.3$ and $-69.6 \pm 1.2\,J\,K^{-1}\,mol^{-1}$ for $[Li(thec9)]^+$ and $[Na(thec9)]^+$, respectively [125].

While ^{13}C NMR spectroscopy shows that Δ and $\Lambda[Pb(thec12)]^{2+}$ also have approximate square antiprismatic stereochemistries analogous to those in Fig. 6, the enantiomerisation rate is much slowed {$k(298.2\,K) = 6550\,s^{-1}$, $\Delta H^\ddagger = 60.4\,kJ\,mol^{-1}$ and $\Delta S^\ddagger = 30.6\,J\,K^{-1}\,mol^{-1}$ in methanol} by comparison with those of their alkali metal analogues [127]. Enantiomerisation of Δ and $\Lambda[Cd(tmec12)]^{2+}$ and its Hg^{2+} and Pb^{2+} analogues for which $k(298.2\,K) = 4130$, 4570 and 565 s^{-1}, $\Delta H^\ddagger = 48.9$, 39.1 and 44.1 kJ mol^{-1}, and $\Delta S^\ddagger = -11.7$, -43.9 and $-44.2\,J\,K^{-1}\,mol^{-1}$, respectively, in methanol are similarly slowed [128]. Over the liquid temperature ranges of methanol and D_2O, $\Lambda[Cd(S\text{-}thpc12)]^{2+}$ and $\Lambda[Pb(S\text{-}thpc12)]^{2+}$ ($\Lambda[Hg(S\text{-}thpc12)]^{2+}$ is insufficiently soluble for ^{13}C NMR studies) exhibit five ^{13}C resonances consistent with the existence of a single approximately square antiprismatic diastereomer in each case [128], probably of a similar structure to that of $\Lambda[Pb(S\text{-}thpc12)]^{2-}$ in the solid state [24]. (Evidently, the rate at which these diastereomers undergo the exchange process analogous to that shown for their alkali metal analogues in Fig. 7 is in the slow exchange limit of the ^{13}C NMR time scale.) The $\log(K/dm^3\,mol^{-1})$ values for $[M(tmec12)]^{2+}$ and $\Lambda[M(S\text{-}thpc12)]^{2+}$ in aqueous solution, where $M^{2+} = Cd^{2+}$, Hg^{2+} and Pb^{2+}, are 12.6, 18.57 and 14.9, and 14.47, 18.63 and 15.74, respectively, which are much higher than those of their alkali metal analogues consistent with stronger coordination in the heavy metal complexes.

Trivalent lanthanide complexes of octadentate ligands formed through the substitution of pendant arms for hydrogen on the four nitrogens of cyclen have generated considerable interest because of their very high stabilities and kinetic inertness [27,129–136] and their consequent potential for use as contrast agents in magnetic resonance imaging [132,137,138] and as nucleases [135,136,139]. Their high stabilities are exemplified by $\log(K/dm^3\,mol^{-1}) = 28.2$, 28.6 and 29.2 for $[Eu(dota)]^{4-}$ and its Tb^{3+} and Lu^{3+} analogues in water at 293.2 K [131]. Enantiomerisation processes similar to those shown in Fig. 6 have been observed for Δ and $\Lambda[La(thec12)]^{3+}$ in ^1H NMR studies in methanol [134], while only the Λ diastereomer is observed for $[La(S\text{-}thpc12)]^{3+}$ and its Eu^{3+} and Lu^{3+} analogues [135]. In the solid state

$[Eu(thpc12)H_2O]^{3+}$ is nine-coordinate with a structure midway between a capped cube and a capped square antiprism when the four α-carbons of the 2-hydroxypropyl arms have R,R,R,S and S,S,S,R chirality [136].

Two interconverting isomers of 1,4,7,10-tetrakis(acetato)-1,4,7,10-tetra-azacyclododecaneneodymium(III), $[Ln(dota)]^-$, where $Ln = La$, Pr, Nd, Sm, Eu, Tb, Dy, Ho, Er, Tm, Yb and Lu, have been detected in solution by ^1H and ^{13}C NMR methods [140]. The relative stabilities of these isomers vary with the lanthanide ion, and $dota^{4-}$ is octadentate in both cases. One isomer has either a square antiprismatic or a capped square antiprismatic structure (when a ninth coordination site is occupied by water) similar to the structures of $[Eu(dota)H_2O]^-$ [133] and its Gd^{3+} [136,141], Y^{3+} [141,142] and Lu^{3+} [143] analogues. The other isomer has a structure close to either a square prism or a capped square prism. Interconversion of Δ and Λ enantiomers (Fig. 9) occurs in both isomers each of which possesses the same macrocyclic ring conformation. For isomerisation of the major to the minor $[Lu(dota)H_2O]^-$ isomer, the minor to the major $[Lu(dota)H_2O]^-$ isomer, and the enantiomerisation of both isomers $k(298.2\ K) = 63.4$, 340 and 18 s^{-1}, $\Delta H^{\ddagger} = 69.3$, 54.4 and 100.5 kJ mol^{-1}, and $\Delta S^{\ddagger} = 22.0$, -14.1 and 116 J K^{-1} mol^{-1}, respectively [140]. The slower and similar enantiomerisation rates for both isomers are ascribed to the rigidity of the coordination cage of $[Lu(dota)H_2O]^-$. Similar isomerisations and enantiomerisations have been observed for $[Yb(dota)H_2O]^-$ [144]. The substitution of a methyl group onto the methylene carbon of each arm to produce R chirality results in the 1,4,7,10-tetrakis((R)-methylacetato)-1,4,7,10-tetraazacyclododecane
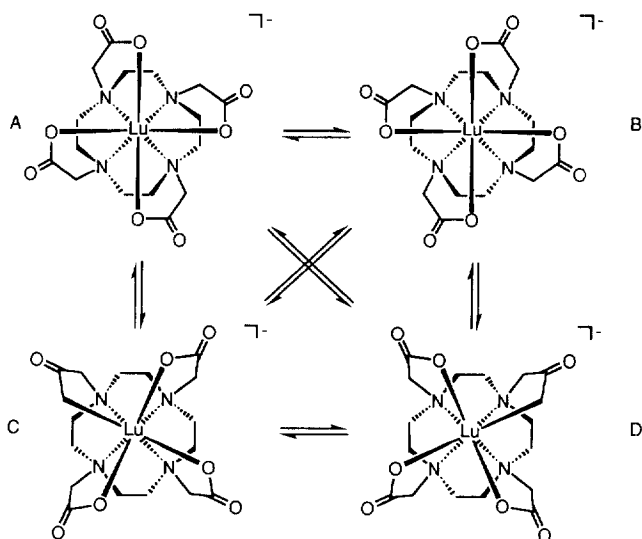

Fig. 9. The enantiomerisation and isomerisation of the major (A and B) and minor (C and D) [Lu(dota)] isomers showing the macrocyclic ring conformations. The capping coordinated water is not shown.

ligand, dotma^{4-}, which forms two [Yb(R-dotma)]$^-$ complexes in solution, in one of which a carboxylate group may be dissociated [129].

When the macrocyclic ring size is increased from 12- to 14-membered, as in 1,4,8,11-tetrakis(2-hydroxyethyl)-1,4,8,11-tetraazacyclotetradecane (thec14), the macrocyclic hole radius increases from $\sim$127 to $\sim$135 pm [28] and the number of configurational isomers with four nitrogens in a plane increases to five designated as *trans* I–V [21]. In methanol, the temperature variation of the natural abundance ^{13}C NMR spectra of [Cd(thec14)]$^{2+}$ and its Hg^{2+} and Pb^{2+} analogues are consistent with thec14 assuming a *trans* III configuration in which two pendant arms are coordinated by the metal centre, and with a transannular exchange process occurring as shown in Fig. 10 [144,145]. When the four 2-hydroxyethyl pendant arms are ^{13}C enriched (99 atom%) the transannular oscillation is more completely character- ised. An unusual aspect of the [Cd(thec14)]$^{2+}$ system is that the coalescence of the two AB quartets in fast exchange results in a singlet ^{13}C resonance because of a reversal of the relative chemical shifts of the two carbons in the monodentate and bidentate pendant arms. This reversal is absent from the Hg^{2+} and Pb^{2-} analogues and a conventional coalescence of two ^{13}C AB quartets to one quartet is observed in fast exchange (Fig. 11).

The kinetic parameters for the transannular mechanism for [Cd(thec14)]$^{2+}$ and its Hg^{2+} and Pb^{2+} analogues are k(298.2 K) = 34 200, 3130 and 11 200 s^{-1}, $\Delta H^{\ddagger}$ = 44.0, 38.0 and 45.4 kJ mol^{-1}, and $\Delta S^{\ddagger}$ = -10.6, -50.6 and -15.2 J K^{-1} mol^{-1}, and the six-coordinate metal ion radii are 95, 102 and 119 pm, respectively [35]. Thus, the increase in size of the metal ion on going from Cd^{2+} to Hg^{2-} results in a decrease in the rate of the exchange process because of the more negative $\Delta S^{\ddagger}$ for [Hg(thec14)]$^{2-}$. This probably indicates that Hg^{2+} is a tighter fit for the molecular hole in thec14 and a more rigid transition state results in which Hg^{2+} is in the tetraaza plane in a stereochemistry similar to that of the postulated intermediate species in Fig. 10. However, [Pb(thec14)]$^{2+}$ does not obey this trend and behaves kinetically as if it is a smaller ion. Lead(II) has two more electrons than Hg^{2+}, and it has been suggested that they act as a stereochemically active lone pair such that the coordination chemistry of Pb^{2+} resembles that of a smaller metal ion in macrocyclic complexes possessing three or more coordinating nitrogens [114,146]. The intermediate shown in Fig. 10 has a similar structure to that of the monodeprotonated Ni^{2+} analogue in the ground state [147] in contrast to the ground
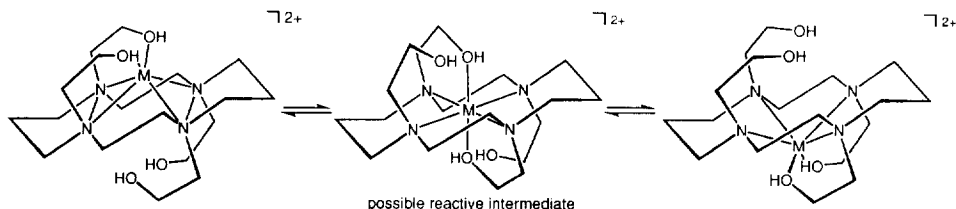

possible reactive intermediate

Fig. 10. The transannular exchange mechanism proposed for [Cd(thec14)]$^{2+}$, and its Hg^{2+} and Pb^{2+} analogues.
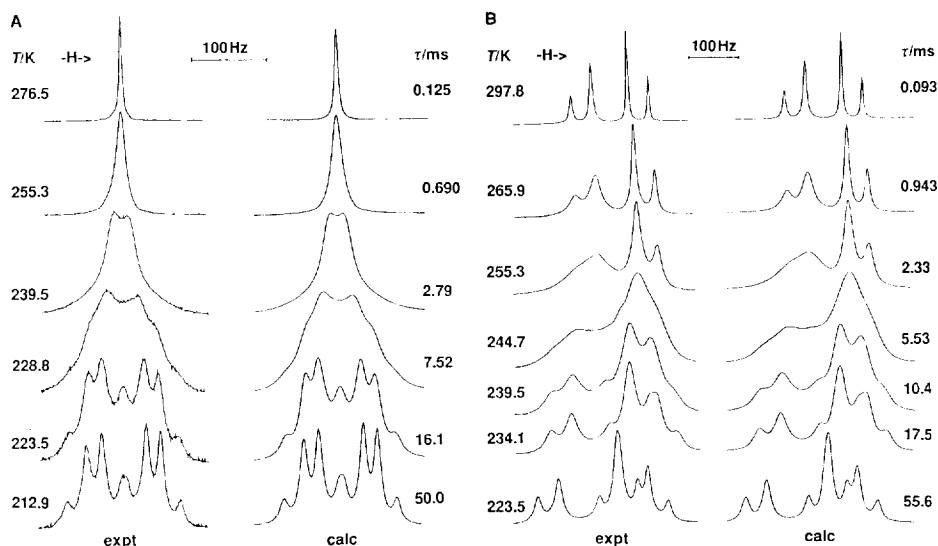
Fig. 11. The exchange modified ^{13}C 75.47 MHz NMR spectra of the 99% ^{13}C enriched 2-hydroxyethyl arms of (A) [Cd(thecl4)]$^{2+}$ and (B) [Pb(thecl4)]$^{2+}$ in CD$_3$OD. The experimental temperatures and derived mean lifetimes of the 2-hydroxyethyl arms in the mono- and bidentate environments appear to the left and right of each figure, respectively. For [Cd(thecl4)]$^{2+}$ $J(^{13}C-^{13}C) = 39.0$ and 39.3 Hz for the downfield and upfield quartets, respectively. For [Pb(thecl4)]$^{2+}$ $J(^{13}C-^{13}C) = 40.5$ and 40.2 Hz for the downfield and upfield quartets, respectively (adapted from Refs. [144] and [145]).

state structures deduced for [Cd(thecl4)]$^{2+}$ and its Hg^{2+} and Pb^{2+} analogues. This difference probably arises because the smaller Ni^{2+}, whose ionic radius is 69 pm, fits more easily into the thecl4 macrocyclic hole.

The mechanism in Fig. 10 contrasts with that proposed for the intramolecular exchange between equivalent trigonal–bipyramidal structures of five-coordinate [M(tmc)X]$^+$ (where M^{2+} = Zn^{2+}, Cd^{2+} or Hg^{2+}, tmc = tetramethylcyclam and X$^-$ is a monodentate anion) which proceeds through a Berry-type mechanism involving rearrangements where tmc is in a folded *trans* I (*cis* I) configuration and X$^-$ occupies an axial site [148,149]. It also contrasts with the mechanism where five-coordinate [Pb(cyclam)X]$^{2+}$ interconverts between folded cyclam *trans* V (*cis* V) R,R,R,R and S,S,S,S configurations [150].

6. Metallocyclodextrins

Cyclodextrins are homochiral cyclic oligosaccharides composed of from six to thirteen α-1,4-linked D-glucopyranose units and are produced by the enzymatic degradation of starch [13–17]. The α-, β- and γ-cyclodextrins are the most plentifully produced and studied, and are composed of six, seven and eight D-glucopyranose units, respectively, as shown in Fig. 12. They possess annular structures whose wide and narrow hydrophilic ends are delineated by O(2)H and O(3)H secondary, and
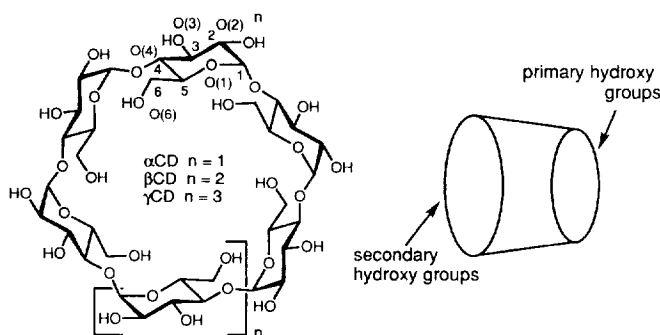
Fig. 12. Schematic representation of α-, β- and γ-cyclodextrin whose internal annular diameters measured from the C(5) hydrogens are 470, 600 and 750 pm, respectively, and 520, 640 and 830 pm measured from the C(3) hydrogens in Corey–Pauling–Koltun models. The depths of the annuli measured between the rings delineated by the primary and secondary hydroxyl groups are 790–800 pm [14,17]. Their representation as a truncated cone is also shown. A substituent drawn at either the narrow or wide end of the cone indicates that it has either replaced a C(6) hydroxyl group, or a C(2) or a C(3) hydroxyl group.

O(6)H primary hydroxy groups, respectively. Their hydrophobic annular interiors are lined with methine and methylene groups and ether oxygens. The size of the cyclodextrin annulus increases with the number of linked D-glucopyranose units so that α-, β- and γ-cyclodextrin can partially or completely "include" a wide range of guests in their annuli to form host–guest complexes, also referred to as "inclusion complexes" [14–17]. The variation in size and the homochirality of the cyclodextrin annuli provide opportunities for both size and chiral discrimination in this inclusion process as indicated by differences in complex stability as the identity of either the guest or the cyclodextrin is varied. Only secondary bonding exists between the cyclodextrin and guest. Nevertheless, the inclusion complexes formed can exhibit considerable stability, and the most stable inclusion complexes are usually formed with substrates possessing some aromatic character.

While cyclodextrins can bind metal ions to form metallocyclodextrins, such complexation is generally weak and involves the formation of hydroxo species [151–153]. Thus, most metallocyclodextrin studies are of modified cyclodextrins where one or more hydroxy groups are substituted by a group which coordinates metal ions to form binary metallocyclodextrins. Subsequently, a guest may include in the cyclodextrin annulus and also coordinate to the metal centre to produce a ternary metallocyclodextrin. This is exemplified by our studies of the formation of binary metallo-6^A-(3-aminopropylamino)-6^A-deoxy-β-cyclodextrins ([M(βCDpn)]$^{2+}$) and their complexation of the tryptophan anion (Trp$^-$) to form the ternary metallocyclo-dextrins ([M(βCDpn)Trp]$^-$) as shown in Fig. 13 and Table 8. The metallo-6^A-(2-(N,N-bis(2-aminoethyl)amino)ethylamino)-6^A-deoxy-β-cyclodextrins, [M(βCDtren)]$^{2+}$ (1 in Fig. 14) and [M(βCDtren)Trp]$^+$ are similarly formed [154–156] (Table 8). The substitution of a βCD primary hydroxy group by $-NH(CH_2)_3NH_2$ and $-NH(CH_2)_2N((CH_2)_2NH_2))_2$ results in strong M^{2+} binding in the binary cyclodextrins which, nevertheless, is not as strong as that in [M(pn)]$^{2+}$
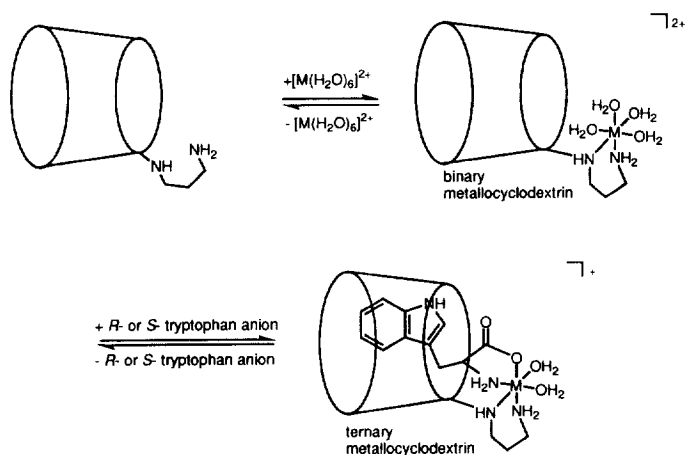
Fig. 13.   The   formation   of   binary   and   ternary   metallocyclodextrins   by 6^A-(3-aminopropylamino)-6^A-deoxy-β-cyclodextrin.

and $[M(tren)]^{2+}$, respectively, where pn is 1,3-diaminopropane and tren is 2,2',2''-triaminotriethylamine [157] (Table 8). This probably reflects the steric hindrance to M^{2+} binding caused by the βCD moiety in βCDpn and βCDtren, and differences in the electron donating powers of the secondary amine groups in βCDpn and βCDtren and primary amine groups in pn and tren. The stability variations for both binary metallocyclodextrins with the nature of M^{2+} arise through a combination of M^{2+} size and ligand field variations, and the higher stabilities of $[M(βCDtren)]^{2+}$, by comparison with those of $[M(βCDpn)]^{2+}$, arise from the tetradentate nature of βCDtren.

The binding of (R)-Trp$^-$ and (S)-Trp$^-$ by $[Ni(βCDpn)]^{2+}$ shows a tenfold discrimination for $[Ni(βCDpn)(S)$-Trp$]^+$ over $[Ni(βCDpn)(R)$-Trp$]^+$ while the Co^{2+} and Cu^{2+} analogues show smaller discriminations, and the Zn^{2+} analogue shows none [154,155]. This effect of M^{2+} on chiral discrimination is coincident with the variation of the ionic radii of six-coordinate Co^{2+}, Ni^{2+}, Cu^{2+} and Zn^{2+} which are 74.5, 69, 73 and 74 pm [35], respectively, and the ligand field imposed constraints in Co^{2+}, Ni^{2+} and Cu^{2+} complex stereochemistry. It is interesting that $[Zn(βCDpn)(R)$-Trp$]^+$ and $[Zn(βCDpn)(S)$-Trp$]^+$ are of the same stability, while the analogous diastereomers for the other three metal ions differ in stability. The absence of ligand field effects in d^{10} Zn^{2+} probably allows more flexibility in the structures of $[Zn(βCDpn)(R)$-Trp$]^+$ and $[Zn(βCDpn)(S)$-Trp$]^+$ and as a result enantioselectivity is decreased. In contrast, the d^9 electronic configuration for similar sized Cu^{2+} imposes a tetragonally distorted octahedral stereochemistry which may impose restrictions on the interaction of the chiral centres of (R)-Trp$^-$ and (S)-Trp$^-$ with the βCDpn moiety and decrease the stability of $[Cu(βCDpn)(R)$-Trp$]^+$ by comparison with that of $[Cu(βCDpn)(S)$-Trp$]^+$. Similar arguments apply in the cases of d^7 Co^{2+} and d^8 Ni^{2+} whose six-coordinate geometries more closely approach regular octahedra. The crucial influence of M^{2+} in chiral

Table 8
Stability constants for 6^A-(3-aminopropylamino)-6^A-deoxy-β-cyclodextrins (βCDpn)[a,b] and 6^A-(2-(N,N-bis(2-aminoethyl)amino)ethylamino)-6^A-deoxy-β-cyclodextrin (βCDtren)[c] metallocyclodextrins and related species in aqueous solution[d]

| Equilibria involving M²⁺ | log(K/dm³ mol⁻¹) | | | |
| | M²⁺ = | | | |
	Co²⁺	Ni²⁺	Cu²⁺	Zn²⁺
M²⁺ + pn = [M(pn)]²⁺		6.31	9.75	-
M²⁺ + tren = [M(tren)]²⁺	12.7	14.6	18.5	14.5
M²⁺ + βCDpn = [M(βCDpn)]²⁺	4.22	5.2	7.35	4.96
M²⁺ + βCDtren = [M(βCDtren)]²⁺	...	11.65	17.29	12.25
M²⁺ + βCDpnH⁺ = [M(βCDpnH)]³⁺	2.5	3.1	3.09	3.0
M²⁺ + βCDtrenH⁺ = [M(βCDtrenH)]³⁺		8.46	11.56	7.92
M²⁺ + Trp = [M(Trp)]⁺	4.41	5.42	8.11	4.90
[M(βCDpn)]²⁺ + (R)-Trp = [M(βCDpn)(R)-Trp]⁺	4.04	4.1	7.85	5.3
[M(βCDpn)]²⁺ + (S)-Trp = [M(βCDpn)(S)-Trp]⁺	4.32	5.1	8.09	5.3
[M(βCDtren)]²⁺ + (R)-Trp = [M(βCDtren)(R)-Trp]⁺		8.2	9.5	8.1
[M(βCDtren)]²⁺ + (S)-Trp = [M(βCDtren)(S)-Trp]⁺	...	8.1	9.4	8.3
[M(βCDtren)]²⁺ + (R)-TrpH = [M(βCDtren)(R)-TrpH]²⁺		4.6	4.3	-
[M(βCDtren)]²⁺ + (S)-TrpH = [M(βCDtren)(S)-TrpH]²⁺		4.3	4.2	
[M(βCDtrenH)]³⁺ + (R)-TrpH = [M(βCDtrenH)(R)-TrpH]³⁺		3.56	4.4	4.82
[M(βCDtrenH)]³⁺ + (S)-TrpH = [M(βCDtrenH)(S)-TrpH]³⁺		3.6	4.4	4.96

Equilibria not involving M²⁺	log(K/dm³ mol⁻¹)			
βCD + (R)-Trp = βCD·(R)-Trp	2.33			
βCD + (S)-Trp = βCD·(S)-Trp	2.33			
βCDpn + (R)-Trp = βCDpn·(R)-Trp	3.41			
βCDpn + (S)-Trp = βCDpn·(S)-Trp	3.40			
βCDtren + (R)-Trp = βCDtren·(R)-Trp	6.36			
βCDtren + (S)-Trp = βCDtren·(S)-Trp	6.5			

[a] Ref. [154].
[b] Ref. [155].
[c] Ref. [156].
[d] At 298.2 K and $I = 0.10$ mol dm⁻³ (NaClO₄).

discrimination in these systems is demonstrated by the lack of chiral discrimination in the βCDpn·(S)-Trp⁻ and βCDpn·(R)-Trp⁻ complexes. A similar variation in chiral discrimination is seen in the analogous phenylalanine anion metallocyclodextrins [158].

The stabilities of the ternary metallocyclodextrins appear to be dominated by three major factors: (i) the hydrophobic interaction between the guest and the βCD annulus interior, (ii) the coordination of the guest to the metal centre, and (iii) the interaction of the guest's chiral centre with the chirality of βCD. It is only when the last factor makes a different contribution in the diastereomeric ternary metallocyclodextrins that thermodynamic enantioselectivity occurs. This is illustrated by the absence of enantioselectivity in [M(βCDtren)(R)-Trp]⁺ and [M(βCDtren)(S)-Trp]⁺ where factors (i) and (ii) appear to dominate despite a
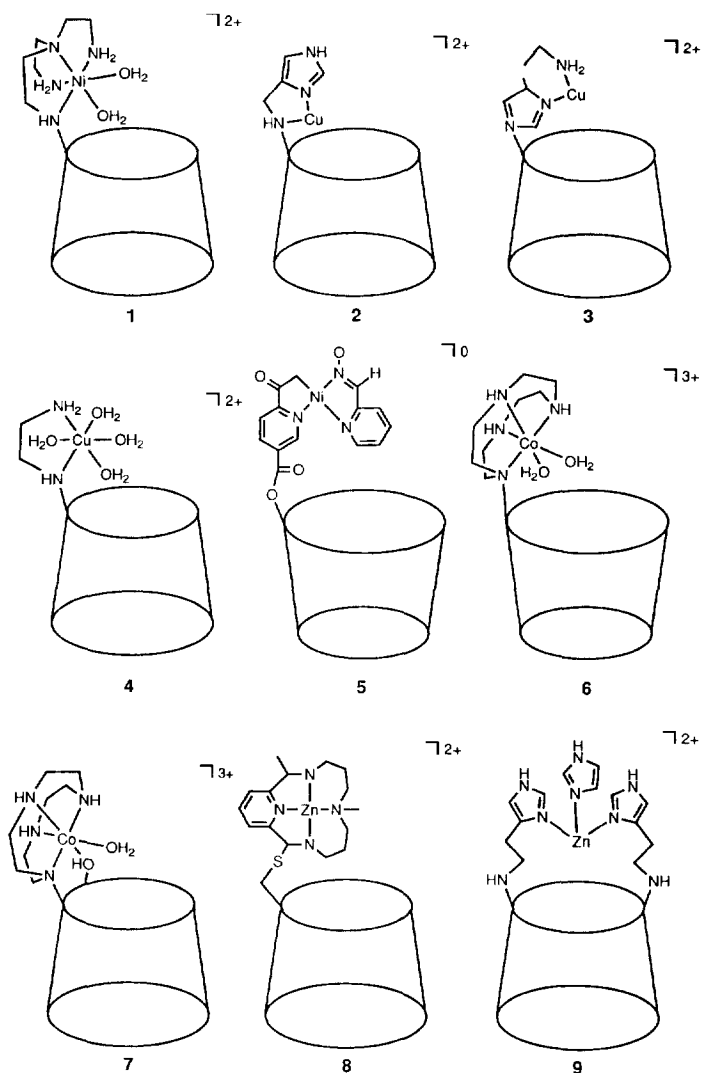
Fig. 14. Schematic representation of some metallocyclodextrins.

considerable increase in stability over that of $[M(\beta CDpn)(R)\text{-}Trp]^+$ and $[M(\beta CDpn)(S)\text{-}Trp]^+$ [156]. The effect of protonation of the guest is shown by $[M(\beta CDtren)(R)\text{-}TrpH]^{2+}$ where monodentate tryptophan (TrpH) does not coordinate as strongly as bidentate Trp^- in the more stable $[M(\beta CDtren)(R)\text{-}Trp]^+$. The $[M(\beta CDpn)(R)\text{-}TrpH]^{2+}$ species is not detected probably because it has a lower stability reflecting the lesser stability of $[M(\beta CDpn)]^{2+}$ by comparison with that of $[M(\beta CDtren)]^{2+}$ where the tetradentate tren substituent coordinates M^{2+} much more strongly than does bidentate pn.

The stabilities of βCDtren·(R)-Trp⁻ and βCDtren·(S)-Trp⁻ are ∼10³ times greater than those for βCDpn·(R)-Trp⁻ and βCDpn·(S)-Trp⁻ which are ∼10 times greater than those for βCD·(R)-Trp⁻ and βCD·(S)-Trp⁻ (Table 8). This variation is attributable to the interaction of the Trp⁻ aminocarboxylate group with the narrow end of the cyclodextrin annulus such that Trp⁻ egress is hindered more than ingress by the substitution of a polyamine at the C(6) site of βCD. The stabilities of [M(βCDtren)(R)-Trp]⁺ and [M(βCDtren)(S)-Trp]⁻ are greater than those of MTrp⁺ and βCDtren·Trp⁻ consistent with the coordination of Trp⁻ by M²⁺ and the interaction of Trp⁻ with the βCD annulus reinforcing each other to stabilise [M(βCDtren)(R)-Trp]⁺ and [M(βCDtren)(S)-Trp]⁺. However, while the stabilities of [M(βCDpn)(R)-Trp]⁺ and [M(βCDpn)(S)-Trp]⁺ are greater than those of βCDpn·Trp⁻, indicating the stabilising effect of coordination of Trp⁻ by M²⁺, they more closely approach those of MTrp⁺ consistent with competition between the Trp⁻ binding effects of the βCD annulus and M²⁺ in these ternary metallocyclodextrins lowering their overall stabilities [157].

Chiral discrimination by metallocyclodextrins has led to their use as chiral discriminating agents in the mobile phase in HPLC enantiomeric separation. This is exemplified by 6ᴬ-[2-(4-imidaz-olyl)ethylamino]-6ᴬ-deoxy-β-cyclodextrincopper(II) (2 in Fig. 14) [159], which complexes the (R)-enantiomers of several aromatic aminoacid anions more strongly than their (S)-enantiomers [160,161]. Such (R)-enantiomers appear to form a more stable ternary metallocyclodextrin because the aromatic moiety of the guest (R)-amino acid anion includes in the βCD annulus while that of the (S)-amino acid anion does not. When 2 is used as the chiral discriminating agent in the mobile phase in HPLC studies, the (R)-enantiomers of tryptophan, phenylalanine and tyrosine elute ahead of the (S)-enantiomers [160,161]. This is because the amino acid anions partition between the mobile aqueous phase and the non-aqueous stationary phase, while the binary and ternary metallocyclodextrins are insoluble in the latter phase. Thus, the enantiomer which forms the most stable ternary metallocyclodextrin spends less time in contact with the HPLC stationary column and elutes first. The enantiomers of the aliphatic amino acids alanine, proline, histidine and leucine were not separated by this HPLC method, probably because the inclusion of an aromatic moiety of the enantiomeric guest in the homochiral cyclodextrin annulus is necessary to engender enantioselectivity.

In contrast to 2, the use of 6ᴬ-[4-(2-aminoethyl)imidazolyl]hist-amino)-6ᴬ-deoxy-β-cyclodextrincopper(II) (3), as a chiral discrimination agent causes (S)-Trp⁻ to elute before (R)-Trp⁻ [162]. This reversal of enantioselectivity arises from the higher stability of the (S)-Trp⁻ ternary metallocyclodextrin which appears to include the aromatic moiety of the guest inside the βCD annulus, while that of its less stable (R)-Trp⁻ analogue does not. The complexation of alanine, phenylalanine and tryptophan anions by 6ᴬ-(2-aminoethylyl-amino)-6ᴬ-deoxy-β-cyclodextrincopper(II) (4), shows no measurable enantioselectivity, but the use of 4 as a chiral discriminating agent in HPLC studies results in (R)-Trp⁻ eluting after (S)-Trp⁻ consistent with a very small enantioselectivity being amplified by chromatography [163].

The ternary metallocyclodextrin, [Ni(βCDpn)(R)-Trp]⁺, shown in Fig. 13 incor-

porates a metal centre in close proximity to a hydrophobic cavity containing a guest. This resembles a Michaelis metalloenzyme complex, as do a range of ternary metallo-cyclodextrins which have been studied as metalloenzyme mimics [164,165]. The first such reported study appears to be the catalysis of the deacyclation of *p*-nitrophenyl acetate by the metallo-α-cyclodextrin **5** (in Fig. 14) [166]. Deacylation is accelerated by $> 10^3$ over the uncatalysed rate, and proceeds through acylation of the pyridinec-arboxaldoxime ligand followed by deacylation of the resulting acetate. Nevertheless, catalysis by **5** is only four-fold more effective than that caused by the pyridinecarboxyaldoximenickel(II) complex. It appears that while the αCD annulus of **5** retains the included *p*-nitrophenyl acetate in close proximity to the attacking pyridinecarboxaldoxime oxygen, significant freedom of movement exists for *p*-nitro-phenyl acetate in the annulus which may diminish the overall catalytic effect of **5**.

The importance of the relative orientations of the metal centre and guest in the ternary metallocyclodextrin is illustrated by the 1000-fold rate acceleration of the deacylation of *p*-nitrophenyl acetate caused by 6^A-(1,4,7,10-tetra-azadodecyl)-6^A-β-cyclodextrincobalt(III) (**6** in Fig. 14), and the smaller acceleration caused by 3^A-(1,4,7,10-tetraazadodecyl)-3^A-β-cyclodextrincobalt(III) (**7**) [167,168]. The probability of the nucleophilic attack on included *p*-nitrophenyl acetate by a hydroxo ligand bound to the Co^{3+} substituent in **7** appears to be decreased by steric hindrance. The $[Co(cyclen)(OH)(H_2O)]^{2+}$ complex has no catalytic effect but 6^A-(1,4,7,10-tetraazadodecyl)-6^A-β-cyclodextrin causes an 8.6 fold deacylation rate acceleration under the same conditions. The influence of the metal centre on catalysis is illustrated by the Ni^{2+}, Cu^{2+} and Zn^{2+} analogues of **6** which cause only 16, 14 and 12-fold accelerations of deacylation of *p*-nitrophenyl acetate, respectively [169].

Michaelis–Menten kinetics are observed for hydrolysis of *p*-nitrophenyl diphenyl-phosphate in the presence of the Zn^{2+} metallo-β-cyclodextrin (**8** in Fig. 14) which accelerates the hydrolysis by a factor of 7 by comparison with the catalysis caused by the complex where the modified βCD substituent is replaced by a methyl group in the tetraaza macrocycle [170]. Zinc(II) appears to act as a bifunctional catalytic centre through simultaneously providing a nucleophilic OH‾ ligand to attack the phosphate ester, and stabilising the development of negatively charged phosphate oxygen through coordination. The increased catalytic effectiveness of the ternary metallocyclodextrin arises from *p*-nitrophenyl diphenylphosphate being localised adjacent to Zn^{2+}. While βCD substituted by diethylenetriamine at C(6) is not a catalyst for the hydrolysis of ribonucleoside 2′,3′-cyclic phosphates, its Zn^{2+} metallo-cyclodextrin accelerates the hydrolysis of the 2′, 3′-cyclic monophosphates of adeno-sine, guanosine, cytosine and uridine, 23-, 28-, 3.5- and 9.6-fold, respectively [171]. This variation is consistent with the purine residues of the first two 2′, 3′-cyclic monophosphates aiding the formation of more stable ternary metallocyclodextrins than do the pyrimidine residues of the second two, and the importance of inclusion of the guest in the metallocyclodextrin cavity in the catalytic process. (It is probable that coordination to Zn^{2+} of the ribonucleoside 2′, 3′-cyclic phosphate guests occurs and increases the stability of the ternary metallocyclodextrin as is the case for the same metallocyclodextrin with a range of different coordinating guests [172].) Smaller accelerations occur for the hydrolysis of ribonucleotide dimers. The ternary

metallocyclodextrin (**9** in Fig. 14) formed when Zn^{2-} is simultaneously coordinated by bis(histamino)-β-cyclodextrin and imidazole resembles the active site of carbonic anhydrase where Zn^{2+} is bound by three imidazoles at the base of a cavity formed by the protein [173]. For CO_2 hydration, **9** is a substantially better catalyst than Zn^{2+} alone, but dehydration of HCO_3^- is not catalysed by **9** probably because HCO_3^- coordinates too strongly to Zn^{2-}.

The study of metallocyclodextrins as enzyme mimics represents an expanding and exciting area of research [164,174–179]. It should be remembered, however, that metalloenzymes have optimised their active site–substrate stereochemistries over millions of years, and it is to be anticipated that significant misalignments of catalytic centre and guest are likely to arise in ternary metallocyclodextrins such that their catalytic activity will often be low relative to that of metalloenzymes.

References

[1] C.J. Pedersen, J. Am. Chem. Soc. 89 (1967) 7017.
[2] C.J. Pedersen, J. Inclusion Phenom. 6 (1988) 337.
[3] J.-M. Lehn, Struct. Bonding (Berlin) 16 (1973) 1.
[4] J.-M. Lehn, J.P. Sauvage, J. Am. Chem. Soc. 97 (1975) 6700.
[5] J.-M. Lehn, Acc. Chem. Res. 11 (1978) 49.
[6] J.-M. Lehn, J. Inclusion Phenom. 6 (1988) 351.
[7] J.-M. Lehn, Supramolecular Chemistry, Concepts and Perspectives, VCH, Weinheim, 1995.
[8] D.J. Cram, Angew. Chem. Int. Ed. Engl. 25 (1986) 1039.
[9] D.J. Cram, J. Inclusion Phenom. 6 (1988) 397.
[10] D.J. Cram, J.M. Cram, Container Molecules and Their Guests, The Royal Society of Chemistry, Cambridge, 1994.
[11] M. Dobler, Ionophores and their Structures, Wiley–Interscience, New York, 1981.
[12] H. Tsukube, in: Y. Inoue, G.W. Gokel (Eds)., Cation Binding by Macrocycles, Marcel Dekker, New York, 1990, p. 497.
[13] M.L. Bender, M. Komiyama, Cyclodextrin Chemistry, Springer Verlag, New York, 1978.
[14] W. Saenger, Angew. Chem. Int. Ed. Engl. 19 (1980) 344.
[15] W. Saenger, Inclusion Compounds 2 (1984) 231.
[16] J. Szejtli, Cyclodextrin Technology, Kluwer, Dordrecht, 1988.
[17] R.J. Clarke, J.H. Coates, S.F. Lincoln, Adv. Carbohyd. Chem. Biochem. 46 (1989) 205.
[18] R. Breslow, Acc. Chem. Res. 28 (1995) 146.
[19] C.J. Easton, S.F. Lincoln, Chem. Soc. Rev. 25 (1996) 163.
[20] J.E. Richman, T.J. Atkins, J. Am. Chem. Soc. 96 (1974) 2268.
[21] B. Bosnich, C.K. Poon, M.L. Tobe, Inorg. Chem. 4 (1965) 1106.
[22] G.A. Melson (Ed.), Coordination Chemistry of Macrocyclic Compounds, Plenum, New York, 1979.
[23] S. Buoen, J. Dale, P. Groth, J. Krane, J. Chem. Soc. Chem. Commun. (1982) 1172.

[24] C.M. Madeyski, J.P. Michael, R.D. Hancock, Inorg. Chem. 23 (1984) 1487.

[25] A.K.W. Stephens, S.F. Lincoln, J. Chem. Soc. Dalton Trans. (1993) 2123.

[26] H. Stetter, W. Frank, Angew. Chem. 88 (1976) 760.

[27] J.F. Desreux, Inorg. Chem. 19 (1980) 1319.

[28] K. Henrick, P.A. Tasker, L. Lindoy, Prog. Inorg. Chem. 33 (1985) 1.

[29] L.F. Lindoy, The Chemistry of Macrocyclic Ligand Complexes, Cambridge University Press, Cambridge, 1989.

[30] G.W. Gokel, Crown Ethers and Cryptands, The Royal Society of Chemistry, Cambridge, UK, 1991.

[31] R.M. Izatt, K. Pawlak, J.S. Bradshaw, R.L. Bruening, Chem. Rev. 91 (1991) 1721.

[32] J.D. Dunitz, P. Seiler, Acta Crystallogr., Sect B: Struct. Crystallogr. Cryst. Chem. B30 (1974) 2739.

[33] P. Seiler, M. Dobler, J.D. Dunitz, Acta Crystallogr., Sect B: Struct. Crystallogr. Cryst. Chem. B30 (1974) 2744.

[34] M. Dobler, J.D. Dunitz, P. Seiler, Acta Crystallogr., Sect B: Struct. Crystallogr. Cryst. Chem. B30 (1974) 2741.

[35] R.D. Shannon, Acta Crystallogr., Sect. A, Cryst. Phys. Diffr. Theory Gen. Crystallogr. A32 (1976) 751.

[36] C.J. Pedersen, J. Am. Chem. Soc. 92 (1970) 386.

[37] H.K. Frensdorf, J. Am. Chem. Soc. 93 (1971) 600.

[38] R.D. Gandour, F.R. Fronczek, V.J. Gatto, C. Miniganti, R.A. Schultz, B.D. White, K.A. Arnold, D. Mazzocchi, S.R. Miller, G.W. Gokel, J. Am. Chem. Soc. 108 (1986) 4078.

[39] P. Groth, Acta Chem. Scand. A35 (1981) 721.

[40] D. Moras, R. Weiss, Acta Crystallogr., Sect B: Struct. Crystallogr. Cryst. Chem. B29 (1973) 400; B29 (1973) 400.

[41] F. Mathieu, B. Metz, D. Moras, R. Weiss, J. Am. Chem. Soc. 100 (1978) 4412.

[42] D. Moras, B. Metz, R. Weiss, Acta Crystallogr., Sect B., Struct. Crystallogr. Cryst. Chem. B29 (1973) 383; B29 (1973) 388.

[43] S.F. Lincoln, E. Horn, M.R. Snow, T.W. Hambley, I.M. Brereton, T.M. Spotswood, J. Chem. Soc. Dalton Trans. (1986) 1075.

[44] R.G. Pearson, J. Am. Chem. Soc. 85 (1963) 3533.

[45] R.G. Pearson, Coord. Chem. Rev. 100 (1990) 403.

[46] R.M. Izatt, R.E. Terry, B.L. Haymore, L.D. Hansen, N.K. Dalley, A.G. Avondet, J.J. Christensen, J. Am. Chem. Soc. 89 (1976) 7620.

[47] H.-J. Buschmann, J. Solution Chem. 16 (1987) 181.

[48] H.-J. Buschmann, J. Inclusion Phenom. Mol. Recogn. Chem. 7 (1989) 581.

[49] G.W. Liesegang, M.M. Farrow, F.A. Vasquez, N. Purdie, E.M. Eyring, J. Am. Chem. Soc. 99 (1977) 3240.

[50] C.C. Chen, S. Petrucci, J. Phys. Chem. 86 (1982) 2601.

[51] S.F. Lincoln, A. White, A.M. Hounslow, J. Chem. Soc. Faraday Trans. 1 83 (1987) 2459.

[52] B.G. Cox, H. Schneider, J.J. Stroka, J. Am. Chem. Soc. 100 (1978) 4746.

[53] B.G. Cox, J. Garcia-Rosas, H. Schneider, J. Am. Chem. Soc. 103 (1981) 1384.

[54] Y.M. Cahen, J.L. Dye, A.I. Popov, J. Phys. Chem. 79 (1975) 1289.

[55] S.F. Lincoln, I.M. Brereton, T.M. Spotswood, J. Chem. Soc. Faraday Trans. 1 81 (1985) 1623.

[56] E. Mei, A.I. Popov, J.L. Dye, J. Am. Chem. Soc. 99 (1977) 6532.

[57] E. Mei, L. Liu, J.L. Dye, A.I. Popov, J. Solution Chem. 6 (1977) 771.

[58] A.I. Popov, Pure Appl. Chem. 51 (1979) 101.

[59] A. Abou-Hamdan, T.W. Hambley, A.M. Hounslow, S.F. Lincoln, J. Chem. Soc. Dalton Trans. (1987) 498.

[60] P. Clarke, S.F. Lincoln, E.R.T. Tiekink, Inorg. Chem. 30 (1991) 2747.

[61] P. Clarke, J.M. Gulbis, S.F. Lincoln, E.R. Tiekink, Inorg. Chem. 31 (1992) 3398.

[62] H. Schneider, S. Rauh, S. Petrucci, J. Phys. Chem. 85 (1981) 2287.

[63] F. Eggers, T. Funck, K.H. Richmann, H. Schneider, E.M. Eyring, S. Petrucci, J. Phys. Chem. 91 (1987) 1961.

[64] H. Schneider, K.H. Richmann, T. Funck, P. Firman, F. Eggers, E.M. Eyring, S. Petrucci, J. Phys. Chem. 92 (1988) 2798.

[65] B.G. Cox, J. Garcia-Rosas, H. Schneider, J. Am. Chem. Soc. 103 (1981) 1054.

[66] Y.M. Cahen, J.L. Dye, A.I. Popov, J. Phys. Chem. 79 (1975) 1292.

[67] S.F. Lincoln, I.M. Brereton, T.M. Spotswood, J. Am. Chem. Soc. 108 (1986) 8134.

[68] S.F. Lincoln, I.M. Brereton, T.M. Spotswood, J. Chem. Soc. Faraday Trans. 1 81 (1985) 1623.

[69] V. Gutmann, Coordination Chemistry in Nonaqueous Solvents, Springer-Verlag, Vienna, 1968.

[70] R.H. Erlich, E. Roach, A.I. Popov, J. Am. Chem. Soc. 92 (1970) 4989.

[71] W.J. DeWitte, A.I. Popov, J. Solution Chem. 5 (1976) 231.

[72] G.W. Gokel, Chem. Soc. Rev. (1992) 39.

[73] K.A. Arnold, L. Echegoyen, F.R. Fronczek, R.D. Gandour, V.J. Gatto, B.D. White, G.W. Gokel, J. Am. Chem. Soc. 109 (1987) 3716.

[74] A. Abou-Hamdan, S.F. Lincoln, M.R. Snow, E.R.T. Tiekink, Aust. J. Chem. 41 (1988) 1363.

[75] T. Rodopoulos, P.-A. Pittet, S.F. Lincoln, J. Chem. Soc. Dalton Trans. 1055 (1993) 2079.

[76] S.F. Lincoln, J. Lucas, J. Chem. Soc. Dalton Trans. (1994) 423.

[77] J. Lucas, S.F. Lincoln, Inorg. Chim. Acta 219 (1994) 217.

[78] B.G. Cox, P. Firman, H. Horst, H. Schneider, Polyhedron 2 (1983) 343.

[79] F.A. Cotton, G. Wilkinson, Advanced Inorganic Chemistry, 5th ed., Interscience, New York, 1988.

[80] H.-J. Buschmann, Inorg. Chim. Acta 102 (1985) 95.

[81] S.F. Lincoln, J. Lucas, T. Rodopolous, Inorg. Chim. Acta 237 (1995) 147.

[82] M. Shamsipur, A.I. Popov, J. Phys. Chem. 90 (1986) 5997.

[83] L. Echegoyen, G.W. Gokel, M.S. Kim, E.M. Eyring, S. Petrucci, J. Phys. Chem. 91 (1987) 3854.

[84] T. Alfheim, J. Dale, P. Groth, K.D. Krautwurst, J. Chem. Soc. Chem. Commun. (1984) 1502.

[85] P. Groth, Acta Chem. Scand. B40 (1985) 59.

[86] P. Groth, Acta Chem. Scand. B40 (1985) 68.

[87] P. Groth, Acta Chem. Scand. B40 (1985) 73.

[88] T. Alfheim, J. Dale, K.D. Krautwurst, Acta Chem. Scand. B40 (1986) 49.

[89] A. Abou-Hamdan, S.F. Lincoln, Inorg. Chem. 30 (1991) 462.

[90] S.F. Lincoln, A.K.W. Stephens, Inorg. Chem. 30 (1991) 3529.

[91] B.G. Cox, J.J. Stroka, I. Schneider, H. Schneider, J. Chem. Soc. Faraday Trans. 1 85 (1989) 187.

[92] E.C. Taylor, A. McKillop, Acc. Chem. Res. 3 (1970) 338.

[93] S.F. Lincoln, E. Horn, M.R. Snow, T. Hambley, I.M. Brereton, T.M. Spotswood, J. Chem. Soc. Dalton Trans. (1986) 1075.

[94] A. Abou-Hamdan, T.W. Hambley, A.M. Hounslow, S.F. Lincoln, J. Chem. Soc. Dalton Trans. (1987) 498.

[95] S.F. Lincoln, A. Abou-Hamdan, Inorg. Chem. 29 (1990) 3584.

[96] S.F. Lincoln, B.J. Steel, I.M. Brereton, T.M. Spotswood, Polyhedron 5 (1986) 1597.

[97] S.F. Lincoln, T. Rodopoulos, Inorg. Chim. Acta 190 (1991) 223.

[98] S.F. Lincoln, T. Rodopoulos, Inorg. Chim. Acta 205 (1993) 23.

[99] P. Clarke, A. Abou-Hamdan, A.M. Hounslow, S.F. Lincoln, Inorg. Chim. Acta 154 (1988) 83.

[100] A. Abou-Hamdan, T.W. Hambley, A.M. Hounslow, S.F. Lincoln, J. Inclusion Phenom. 5 (1987) 137.

[101] P. Clarke, S.F. Lincoln, E.R.T. Tiekink, Inorg. Chem. 30 (1991) 2747.

[102] P. Clarke, J.M. Gulbis, S.F. Lincoln, E.R.T. Tiekink, Inorg. Chem. 31 (1992) 3398.

[103] R. Dhillon, S.F. Lincoln, Aust. J. Chem. 47 (1994) 123.

[104] S.F. Lincoln, A.K.W. Stephens, Inorg. Chem. 31 (1992) 5067.

[105] M. Shamsipur, A.I. Popov, Inorg. Chim. Acta 43 (1980) 243.

[106] R.D. Boss, A.I. Popov, Inorg. Chem. 25 (1986) 1747.

[107] S. Kulstad, L.A. Malmsten, J. Inorg. Nucl. Chem. 42 (1980) 573.

[108] B. Moras, B. Metz, M. Herceg, R. Weiss, Bull. Soc. Chim. Fr. (1972) 551.

[109] R.S. Dhillon, P.A. Duckworth, S.F. Lincoln, A.K.W. Stephens, Inorg. Chim. Acta 215 (1994) 79.

[110] P.A. Duckworth, S.F. Lincoln, J. Lucas, Inorg. Chim. Acta 188 (1991) 55.

[111] R.D. Hancock, in: A.F. Williams, A. Floriani, A.E. Merbach (Eds.), Perspectives in Coordination Chemistry, VCH, Cambridge, 1992, p. 129.

[112] S. Buøen, J. Dale, P. Groth, J. Krane, J. Chem. Soc. Chem. Commun. (1982) 1172.

[113] A.K.W. Stephens, S.F. Lincoln, J. Chem. Soc. Dalton Trans. (1993) 2123.

[114] R.D. Hancock. M.S. Shaikjee, S.M. Dobson, J.C.A. Boeyens, Inorg. Chim. Acta 154 (1988) 229–238.
[115] H. Stetter, W. Frank, R. Mertens, Tetrahedron 37 (1981) 767.
[116] M.L. Turonek, P. Clarke, G.S. Laurence, S.F. Lincoln, P.-A. Pittet, S. Politis, K.P. Wainwright, Inorg. Chem. 32 (1993) 2195.
[117] R. Dhillon, A.K.W. Stephens, S.L. Whitbread, S.F. Lincoln, K.P. Wainwright, J. Chem. Soc. Chem. Commun. (1995) 97.
[118] S.L. Whitbread. S. Polites, A.K.W. Stephens, J.B. Lucas, R. Dhillon, S.F. Lincoln, K.P. Wainwright, J. Chem. Soc. Dalton Trans. (1996) 1379.
[119] A.K.W. Stephens, R.S. Dhillon, S.E. Madbak, S.L. Whitbread, S.F. Lincoln, Inorg. Chem. 35 (1996) 2019.
[120] R.S. Dhillon, S.E. Madbak, F.G. Ciccone, M.A. Buntine, S.F. Lincoln, K.P. Wainwright, J. Am. Chem. Soc. 119 (1997) 6126.
[121] P. Groth, Acta Chem. Scand. A37 (1983) 283.
[122] S. Buøen, J. Dale, J. Krane, Acta Chem. Scand. B38 (1984) 773.
[123] Gaussian 94, Revision C.3, M.J. Frisch, G.W. Trucks, H.B. Schlegel, P.M.W. Gill, B.G. Johnson, M.A. Robb, J.R. Cheeseman, T. Keith, G.A. Petersson, J.A. Montgomery, K. Raghavachari, M.A. Al-Laham, V.G. Zakrzewski, J.V. Ortiz, J.B. Foresman, J. Cioslowski, B.B. Stefanov, A. Nanayakkara, M. Challacombe, C.Y. Peng, P.Y. Ayala, W. Chen, M.W. Wong, J.L. Andres, E.S. Replogle, R. Gomperts, R.L. Martin, D.J. Fox, J.S. Binkley, D.J. Defrees, J. Baker, J.P. Stewart, M. Head-Gordon, C. Gonzalez, J.A. Pople, Gaussian, Inc., Pittsburgh, PA, 1995.
[124] R. Luckay, J.H. Reibenspies, R.D. Hancock, J. Chem. Soc. Chem. Commun. (1995) 2365.
[125] S.L. Whitbread, J. Weeks, P. Valente, M.A. Buntine, S.F. Lincoln, K.P. Wainwright, Aust. J. Chem. to be published.
[126] I. Fallis, L.J. Farrugia, N.M. Macdonald, R.D. Peacock, Inorg. Chem. 32 (1993) 779.
[127] S.F. Lincoln, G.S. Laurence, P.-A. Pittet, M. Turonek, K.P. Wainwright, J. Chem. Soc. Chem. Commun. (1991) 1205.
[128] A.K.W. Stephens, R. Dhillon, S.F. Lincoln, K.P. Wainwright, Inorg. Chim. Acta 236 (1995) 185.
[129] H.G. Brittain, J.F. Desreux, Inorg. Chem. 23 (1984) 4459.
[130] M.R. Spirlet, J. Rebizant. J.F. Desreux, M.-F. Loncin, Inorg. Chem. 23 (1984) 359.
[131] M.F. Loncin, J.F. Desreux, E. Merciny, Inorg. Chem. 25 (1986) 2646.
[132] J.F. Desreux, P.P. Barthlemy, Nucl. Med. Biol. 15 (1988) 9.
[133] J.-P. Dubost, M. Leger, M.-H. Langlois, D. Meyer, M. Schaefer, C. R. Acad. Sci. Paris, Ser. 2 312 (1991) 349.
[134] S. Aime, M. Botta, G. Ermondi, Inorg. Chem. 31 (1992) 4291.
[135] J.R. Morrow, K.O.A. Chin, Inorg. Chem. 32 (1993) 3357.
[136] K.O.A. Chin, J.R. Morrow, C.H. Lake, M.R. Churchill, Inorg. Chem. 33 (1994) 656.
[137] R.B. Laufer, Chem. Rev. 87 (1987) 901.
[138] D. Parker, Chem. Soc. Rev. 19 (1990) 271.
[139] J.R. Morrow, K. Aures. D. Epstein, J. Chem. Soc. Chem. Commun. (1995) 2431.
[140] S. Aime, A. Barge, M. Botta, M. Fasano. J.D. Ayala, G. Bombieri, Inorg. Chim. Acta 246 (1996) 423.
[141] C.A. Chang, L.C. Francesconi, K. Kumar, M.F. Malley, J.G. Goutas, M.F. Tweedle, D.W. Lee, J.G. Wilson, Inorg. Chem. 32 (1993) 3501.
[142] D. Parker, K. Pulokkody, F.C. Smith, A. Batsanova, J.A.K. Howard, J. Chem. Soc. Dalton Trans. (1994) 689.
[143] V. Jaques, J.F. Desreux, Inorg. Chem. 33 (1994) 4048.
[144] P. Clarke, A.M. Hounslow, R.A. Keough. S.F. Lincoln, K.P. Wainwright, Inorg. Chem. 29 (1990) 1793.
[145] P. Clarke, S.F. Lincoln, K.P. Wainwright, Inorg. Chem. 30 (1991) 134.
[146] R.D. Hancock, R. Bhavan, P.W. Wade, J.C.A. Boeyens, S.M. Dobson, Inorg. Chem. 28 (1989) 187.
[147] R.W. Hay, M.P. Pujari, W.T. Moodie, S. Craig, D.T. Richens, A. Perotti, L. Ungaretti, J. Chem. Soc. Dalton Trans. (1986) 953.
[148] N.W. Alcock, N. Herron, P. Moore, J. Chem. Soc. Dalton Trans. (1978) 1282.

[149] N.W. Alcock, E.H. Curson, N. Herron, P. Moore, J. Chem. Soc. Dalton Trans. (1979) 1987.

[150] N.W. Alcock, N. Herron, P. Moore, J. Chem. Soc. Dalton Trans. (1979) 1487.

[151] K. Mochida, Y. Matsui, Chem. Lett. (1976) 963.

[152] M. McNamara, N.R. Russell, J. Inclusion Phenom. Mol. Recogn. 13 (1992) 145.

[153] R. Fuchs, N. Habermann, P. Klüfers, Angew. Chem. Int. Ed. Engl. 32 (1993) 852.

[154] S.E. Brown, J.H. Coates, C.J. Easton, S.J. van Eyk, S.F. Lincoln, B.L. May, M.A. Stile, C.B. Whalland, M.L. Williams, J. Chem. Soc. Chem. Commun. (1994) 47.

[155] S.E. Brown, J.H. Coates, C.J. Easton, S.F. Lincoln, J. Chem. Soc. Faraday Trans. 90 (1994) 739.

[156] C.A. Haskard, C.J. Easton, B.L. May, S.F. Lincoln, Inorg. Chem. 35 (1996) 1059.

[157] A.E. Martell, R.M. Smith, Critical Stability Constants, vol. 2, Plenum Press, New York, 1975.

[158] S.E. Brown, C.A. Haskard, C.J. Easton, S.F. Lincoln, J. Chem. Soc. Faraday Trans. 91 (1995) 1013; 91 (1995) 4335.

[159] R.P. Bonomo, V. Cucinotta, F. D'Alessandro, G. Impellizzeri, G. Maccarrone, G. Vecchio, E. Rizzarelli, Inorg. Chem. 30 (1991) 2708.

[160] G. Impellizzeri, G. Maccarrone, E. Rizzarelli, G. Vecchio, R. Corradini, R. Marchelli, Angew. Chem. Int. Ed. Engl. 30 (1991) 1348.

[161] R. Corradini, A. Dossena, G. Impellizzeri, G. Maccarrone, R. Marchelli, E. Rizzarelli, G. Sartor, G. Vecchio, J. Am. Chem. Soc. 116 (1994) 10267.

[162] V. Cucinotta, F. D'Alessandro, G. Impellizzeri, G. Vecchio, J. Chem. Soc. Chem. Commun. (1992) 1743.

[163] R.P. Bonomo, V. Cucinotta, F. D'Alessandro, G. Impellizzeri, G. Maccarrone, E. Rizzarelli, G. Vecchio, J. Inclusion Phenom. Mol. Recogn. Chem. 15 (1993) 167.

[164] R. Breslow, Acc. Chem. Res. 28 (1995) 146.

[165] Y. Murakami, J. Kikuchi, Y. Hisaeda, O. Hayashida, Chem. Rev. 96 (1996) 721.

[166] R. Breslow, L.E. Overman, J. Am. Chem. Soc. 92 (1970) 1075.

[167] E.U. Akkaya, A.W. Czarnik, J. Am. Chem. Soc. 110 (1988) 8553.

[168] E.U. Akkaya, A.W. Czarnik, J. Phys. Org. Chem. 5 (1992) 540.

[169] M.I. Rosenthal, A.W. Czarnik, J. Inclusion Phenom. Mol. Recogn. 10 (1991) 119.

[170] R. Breslow, S. Singh, Bioorg. Chem. 16 (1988) 408.

[171] M. Komiyama, Y. Matsumoto, Chem. Lett. (1989) 719.

[172] I. Tabushi, N. Shimizu, T. Sugimoto, M. Shiozuka, K. Yamamura, J. Am. Chem. Soc. 99 (1977) 7100.

[173] I. Tabushi, Y. Kuroda, J. Am. Chem. Soc. 106 (1984) 4580.

[174] R. Fornasier, E. Scarpa, P. Scrimin, P. Tecilla, U. Tonellato, J. Inclusion Phenom. Mol. Recogn. Chem. 14 (1992) 205.

[175] Y. Matsui, T. Yokoi, K. Mochida, Chem. Lett. (1976) 1037.

[176] H.-J. Schneider, F. Xiao, J. Chem. Soc. Perkin Trans. II (1992) 387.

[177] A.W. Coleman, C.-C. Ling, M. Miocque, Angew. Chem. Int. Ed. Engl. 31 (1992) 1381.

[178] Y. Kuroda, T. Hiroshige, T. Sera, Y. Shiriwa, H. Tanaka, H. Ogoshi, J. Am. Chem. Soc. 111 (1989) 1912.

[179] Y. Kuroda, T. Hiroshige, H. Ogoshi, J. Chem. Soc. Chem. Commun. (1990) 1594.